Arabian Journal of Chemistry (2020) **13**, 6379–6394

King Saud University

Arabian Journal of Chemistry

www.ksu.edu.sa
www.sciencedirect.com

ORIGINAL ARTICLE

In vitro biological studies of heteroleptic Ag(I) and Cu(I) unsymmetrical N,N′-diarylformamidine dithiocarbamate phosphine complexes; the effect of the metal center

Segun D. Oladipo [a], **Chunderika Mocktar** [b], **Bernard Omondi** [c,*]

[a] *School of Chemistry and Physics, Westville Campus, University of Kwazulu-Natal, Private Bag X54001, Durban 4000, South Africa*
[b] *Discipline of Pharmaceutical Sciences, School of Health Sciences, University of Kwazulu-Natal, Private Bag X54001, Durban 4000, South Africa*
[c] *School of Chemistry and Physics, Pietermaritzburg Campus, University of Kwazulu-Natal, Private Bag X01, Scottsville 3209, South Africa*

Received 20 April 2020; revised 28 May 2020; accepted 29 May 2020
Available online 20 June 2020

KEYWORDS

Copper(I) complexes;
Silver (I) complexes;
Dithiocarbamate;
Antioxidant;
In vitro antibacterial activity

Abstract A series of five dithiocarbamate and their respective Ag(I) and Cu(I) triphenylphosphine complexes of the general formula [Ag/Cu(PPh_3)$_2$**L**] were synthesized and characterized. The dithiocarbamate ligands were synthesized from formamidines with substituents in the 2 and/or 6 positions of the phenyl rings, intentionally keeping substituents on one ring different from those of the second phenyl ring while investigating the structure-activity relationship of Ag(I) and Cu(I) dithiocarbamate complexes. All Ag(I) and Cu(I) complexes with the general formula [Ag(PPh_3)$_2$**L**] (**1–5) or** [Cu(PPh_3)$_2$**L**] (**6–10**), displayed distorted tetrahedral geometry around the metal centers with coordination *via* two S atoms of the dithiocarbamate ligand and two P atoms from the PPh_3 units. Complexes **1–5** showed better inhibition values against Gram-positive, *Staphylococcus aureus* (methicillin resistant) and *Staphylococcus aureus* than the standard used, ciprofloxacin. Complexes **1** and **2** generally had good activity against all bacterial strains but were not active against *Salmonella typhimurium*. All Cu(I) complexes were either of low activity or inactive against all bacterial strains tested. Complex **2** was found to be more active with IC_{50} values of 1.34×10^{-3} mM and 0.25 mM as agents for antioxidant activity against DPPH and NO free radical scavengers,

* Corresponding author.
E-mail address: owaga@ukzn.ac.za (B. Omondi).
URLs: https://orcid.org/0000-0003-2489-1752 (S.D. Oladipo), http://orcid.org/0000-0002-3003-6712 (B. Omondi).
Peer review under responsibility of King Saud University.

Production and hosting by Elsevier

https://doi.org/10.1016/j.arabjc.2020.05.039

respectively. The metal center played a vital role in their biological activity as the Ag(I) complexes displayed better antibacterial and antioxidant activity than Cu(I) complexes.

1. Introduction

The chemistry of metal dithiocarbamates is well known (Barba et al., 2012; Cardell et al., 2006; Halimehjani et al., 2015; Hogarth, 2012; Oladipo and Omondi, 2020) and has aroused interest in electrochemical (Wilton-Ely et al., 2008), magnetic (Okubo et al., 2010), and optical studies (Semeniuc et al., 2010; Tan et al., 2013; Kumar et al., 2014a, 2014b). Besides, they have been used as single-source precursors in the syntheses of metal sulfide nanoparticles (Bruce et al., 2007; Mthethwa et al., 2009; Bera et al., 2010; Maji et al., 2012; Ramasamy et al., 2013; Oladipo and Omondi, 2020) as biological agents (Güzel and Salman, 2006; Rani et al., 2014; Islam et al., 2016), in metallurgy (Abramov and Forssberg, 2005), in the vulcanization of rubber and in agriculture as pesticides (Mohamed et al., 2009). The interest in the chemistry for dithiocarbamate ligands arises from the ease of their functionalization, which may lead to a variety of structural architectures and controlled physical properties. As versatile ligands, they are capable of coordinating to different metals in diverse bonding modes (Hogarth et al., 2012) while also being used as coligands in the synthesis of heteroleptic complexes (Afzaal et al., 2011; Gupta et al., 2014). Such complexes are of interest structurally in coordination chemistry and in bio-inorganic chemistry (Ekennia et al., 2016; El-Sherif and Jeragh, 2007).

Ag(I) complexes of heteroatom ligands such as those with S and P donor atoms have recently attracted great interest biologically due to the relevance of metal-sulfur systems and their interactions with molecules within living organisms (Ahmad et al., 2006). Such complexes have found applications as antitumor (Berners-Price et al., 1988; McKeage et al., 1998; Hadjikakou et al., 2008), and as antibacterial agents (Nomiya et al., 2004; Isab and Wazeer, 2007; Hanif et al., 2008) with biological activity attributed to not only the metal center, but also the coordinating ligand. The presence of heteroatoms can be from the same ligand (e.g. *N,O; N,P* etc) or each atom could be from separate ligands. The latter case is what leads to heteroleptic complexes. Dithiocarbamates in such a case an obvious source of the S atom while a coligand like phosphines would be a source of your P atoms. Only a few studies of heteroleptic Cu(I) dithiocarbamate phosphines as potential biological agents are reported to date (Rajput et al., 2012) with most of the studies of the complexes being on optical properties of the excellent photoluminescing dithiocarbamates (Kutal, 1990; Ford et al., 1999). This has rendered them useful in applications in energy conversion especially in solar cells (Sandroni et al., 2013, 2014), light emission in electrochemical devices (Wang et al., 2005; Elie et al., 2016), imaging in biological cells (Lim et al., 2006; Xin et al., 2014), and in sensors (Yang et al., 2005; Domaille et al., 2010). Diethyldithiocarbamate and its disulfiram derivatives along with the copper complex are know to inhibit superoxide dismutase and in rodents have been used *in vivo* for the treatment of oxygen toxicity to the central nervous system (Liu et al., 1996). Cu(I) complexes have also been reported to possess good catalytic properties (Melekhova et al., 2017a, 2017b) with their physicochemical properties being studied theoretically in literature (Melekhova et al., 2017a, 2017b, 2015).

Dithiocarbamate ligands on their own readily react with Ag (I) and Cu(I) salts to form a variety of complexes and clusters with varying nuclearities and architectures (Huang et al., 2007; Costa et al., 2011; Barreiro et al., 2013; Kumar et al., 2014a, 2014b). Other ligands with strong σ-donor and π-acceptors such as bulky phosphine can be used to control the multinuclearity in the Ag(I) and Cu(I) dithiocarbamate complexes. Bulky phosphine ligands can stabilize the + 1 oxidation states of silver and copper and in the process, impose tetrahedral geometry around the metal centers.

Formamidines as part of the dithiocarbamates, have been shown to have good cytotoxicity against some tumour cell lines (Soliman et al., 2016). Besides, formamidine derivatives and their related compounds have been extensively used as biologically active complexing and analytical reagents (Liu et al., 1996; Ren et al., 1998; Chisholm et al., 1999; Clerac et al., 2001). The ease of the synthesis of formamidine ligands and their derivatives has driven their studies to get more biologically active ligands. We have previously reported on the biological studies of the Ni(II) and Cu(II) dithiocarbamate complexes which showed interesting results (Oladipo et al., 2019). To advance these studies, we have introduced phosphines to investigate if this might enhance the biological activities of the complexes (Frezza et al., 2011; Nazarov and Dyson, 2011; Samouei et al., 2011; Kamatchi et al., 2012; Sampath et al., 2013; Fereidoonnezhad et al., 2017).

We have also used Cu(I) and Ag(I) to try and draw conclusions on the influence of the nature of metal center in bioactivity. Besides the action of the ligand we hope to see the extent of lability of the metal centers via the bioactivity. We therefore report the synthesis, structural characterization and *in vitro* biological studies of heteroleptic Ag(I) and Cu(I) N,N′-diarylformamidine dithiocarbamate phosphine complexes. The antimicrobial potentials of the metal complexes were evaluated against Gram-positive bacterial strains *Staphylococcus aureus* (methicillin resistant) and *Staphylococcus aureus* and Gram-negative bacterial strains *Escherichia coli*, *Salmonella typhimurium, Pseudomonas aeruginosa,* and K *pneumonia,* while the antioxidant potentials were evaluated using the 2,2,1-diphenyl-1-picrylhydrazyl (DPPH) and Nitric oxide (NO) scavenging assays.

2. Materials and methods

All solvents (ACS reagent grades ≥ 99.5%) were obtained from Sigma-Aldrich and used as obtained without further purification. Reagents: 2,6-diisopropylaniline (97%), 2,6-dimethylaniline (99%), 2,4,6-trimethylaniline (98%), 2,6-dichloroaniline (98%), 2-bromoaniline (98%), triphenylphosphine (99%), triethyl orthoformate (99%) and carbon disulfide were also obtained from Sigma Aldrich. Metal salts: $AgNO_3$

(≥99.0%) and $Cu(NO3)_2{\cdot}3H_2O$ (99.0%) were obtained from Promark Chemicals South Africa.

The melting point of the complexes were recorded using Electrothermal (9100). ^1H and ^{13}C NMR spectra were recorded at 25 °C on a Bruker AvanceIII 400 MHz spectrometer. Both ^1H NMR and ^{13}C NMR data were recorded in either $CDCl_3$ referenced to the residual $CDCl_3$ peaks at δ 7.26 and δ 77.00 ppm or $(CD_3)_2SO$ (DMSO) referenced to the residual $(CD_3)_2SO$ peaks at δ 2.50 and δ 39.52 ppm respectively. Elemental analyses were recorded on a Vario elemental EL cube CHNS analyzer. IR spectra were obtained on a PerkinElmer Universal ATR spectrum 100 FT-IR spectrometer and UV–Vis absorption spectra were recorded on Shimadzu UV–vis-NIR spectrophotometer.

3. General synthesis procedure

3.1. Syntheses of complexes

The metal salts, $[Ag/Cu(PPh_3)_2NO_3]$, used in this study were synthesized following a procedure from the literature (Gysling and Kubas, 1979) with slight modifications. We reported the synthesis of potassium dithiocarbamate salts **L1** – **L5** (Oladipo et al., 2020) and the complexes were prepared by following the general literature procedure (Rajput et al., 2012). 1 mmol of **L1** – **L5** were dissolved in 20 ml acetonitrile in a round bottom flask. To the resultant solution, 1 mmol of $[Ag/Cu(PPh_3)_2NO_3]$ dissolved in 10 ml of dichloromethane was added drop-wise and stirred for 1 hr at room temperature. The resultant yellow solids were collected by filtration, washed three times with ethanol and then twice with diethyl ether. The pure products were dried in the oven at 40 °C and stored in a desiccator.

*3.1.1. Synthesis of [Ag(PPh$_3$)$_2$L1], **1***

The reaction of **L1** (0.25 g, 7 mmol) and $[Ag(PPh_3)_2$**L1**] (0.30 g, 7 mmol) in acetonitrile furnished complex **1** as a yellow powder. Yield: (0.40 g, 73%). Melting point: 204–205 °C. ^1H NMR ($CDCl_3$, 400 MHz): δ (ppm) 2.30 (s, 6H, CH_3-Ar), 6.85 (t, 1H, $J_{H,H}$ = 8.08 Hz, Ar-H), 7.12 (d, 2H, $J_{H,H}$ = 7.16 Hz, Ar-H), 7.22 (d, 3H, $J_{H,H}$ = 7.60 Hz, Ar-H), 7.25 (d, 12H, $J_{H,H}$ = 7.46 Hz, PPh_3), 7.36 (m, 18H, $J_{H,H}$ = 7.63 Hz, PPh_3), 9.86 (s, 1H, —CH═N). ^{13}C NMR ($CDCl_3$, 100 MHz) δ (ppm): 17.98, 18.94, 124.04, 127.39, 127.87, 128.02, 128.06, 128.33, 128.63, 128.72, 129.84, 133.31, 133.53, 133.79, 133.96, 135.89, 139.31, 145.79, 153.90 and 218.84. ^{13}P NMR (121.50 MHz, $CDCl_3$): δ = 7.04 IR υ (cm^{-1}): 2919(w), 1640(s), 1477(s), 1092(s), 877(s), 422(m), 504(m). UV–Vis ($CHCl_3$, λ_{max}, nm), 292 and 338. Anal. calcd for $AgC_{52}H_{44}Cl_2N_2P_2S_2$: C, 62.35; H, 4.43; N, 2.80; S, 6.40. Found: C, 62.76; H, 5.053; N, 2.88; S, 6.38.

*3.1.2. Synthesis of [Ag(PPh$_3$)$_2$L2] **2***

The reaction of **L2** (0.33 g, 7 mmol) and $[Ag(PPh_3)_2$**L2**] (0.30 g, 7 mmol) in acetonitrile furnished complex **2** as a yellow powder. Yield: (0.45 g, 71%). Melting point: 194–195 °C. ^1H NMR ($CDCl_3$, 400 MHz): δ (ppm) 1.09 (d, 6H, $J_{H,H}$ = 6.72 Hz, CH_3-CH), 1.25 (d, 6H, $J_{H,H}$ = 6.72 Hz, CH_3-CH), 2.96 (m, 2H, $J_{H,H}$ = 6.64 Hz, CH-CH_3), 6.86 (t, 1H, $J_{H,H}$ = 8.04 Hz, Ar-H), 7.21 (s, 2H, Ar-H), 7.22 (d, 3H, $J_{H,H}$ = 7.36 Hz, Ar-H), 7.26 (t, 12H, $J_{H,H}$ = 7.54 Hz, PPh_3), 7.36 (m, 18H, $J_{H,H}$ = 7.51 Hz, PPh_3), 10.14 (s, 1H, —CH═N). ^{13}C NMR ($CDCl_3$, 100 MHz) δ (ppm): 0.24.59, 24.67, 28.77, 123.96, 127.48, 128.23, 128.64, 128.73, 128.97, 129.86, 133.15, 133.38, 133.80, 133.96, 135.93, 145.88, 146.07, 155.80 and 220.58. ^{13}P NMR (121.50 MHZ, $CDCl_3$): δ = 7.02. IR υ (cm^{-1}): 2950(w), 1634(s), 1477(s), 1093(s), 877(s), 421(m), 501(m). UV–Vis ($CHCl_3$, λ_{max}, nm), 289 and 339. Anal. calcd for $AgC_{56}H_{52}Cl_2N_2P_2S_2$: C, 63.58; H, 4.95; N, 2.65; S, 6.06. Found: C, 62.70; H, 5.053; N, 2.49; S, 5.24.

*3.1.3. Synthesis of [Ag(PPh$_3$)$_2$DL3] **3***

The reaction of **L3** (0.27 g, 7 mmol) and $[Ag(PPh_3)_2$**L3**] (0.30 g, 7 mmol) in acetonitrile furnished complex **3** as a yellow powder. Yield: (0.43 g, 76%). Melting point: 192 – 193 °C. ^1H NMR ($CDCl_3$, 400 MHz): δ (ppm) 2.26 (s, 9H, CH_3-Ar), 6.85 (t, 1H, $J_{H,H}$ = 8.04 Hz, Ar-H), 6.94 (s, 3H, Ar-H), 7.23 (d, 3H, $J_{H,H}$ = 8.01 Hz, Ar-H), 7.26 (d, 11H, $J_{H,H}$ = 7.04 Hz, PPh_3), 7.36 (m, 19H, $J_{H,H}$ = 7.96 Hz, PPh_3), 9.86 (s, 1H, —CH═N). ^{13}C NMR ($CDCl_3$, 100 MHz) δ (ppm): 17.86, 21.37, 124.00, 127.42, 127.96, 128.62, 128.71, 129.04, 129.82, 133.32, 133.54, 133.80, 133.96, 135.42, 136.68, 137.80, 145.90, 154.01 and 219.07. ^{13}P NMR (121.50 MHZ, $CDCl_3$): δ = 7.02. IR υ (cm^{-1}): 2950(w), 1639(s), 1479(s), 1094(s), 878(s), 418(m), 501(m). UV–Vis ($CHCl_3$, λ_{max}, nm), 292 and 338. Anal. calcd for $AgC_{53}H_{46}Cl_2N_2P_2S_2$: C, 62.67; H, 4.56; N, 2.75; S, 6.31. Found: C, 62.88; H, 4.76; N, 2.88; S, 6.24.

*3.1.4. Synthesis of [Ag(PPh$_3$)$_2$DL4] **4***

The reaction of **L4** (0.28 g, 7 mmol) and $[Ag(PPh_3)_2$**L4**] (0.30 g, 7 mmol) in acetonitrile furnished complex **4** as a yellow powder. Yield: (0.45 g, 77%). Melting point: 190–192 °C. ^1H NMR ($CDCl_3$, 400 MHz): δ (ppm) 2.26 (s, 6H, CH_3-Ar), 6.91 (t, 1H, $J_{H,H}$ = 7.44 Hz, Ar-H), 6.95 (d, 1H, $J_{H,H}$ = 7.86 Hz, Ar-H), 7.12 (t, 2H, $J_{H,H}$ = 7.56 Hz, Ar-H), 7.19 (m, 2H, $J_{H,H}$ = 6.84 Hz, Ar-H), 7.26 (t, 13H, $J_{H,H}$ = 7.16 Hz, PPh_3), 7.36 (m, 17H, $J_{H,H}$ = 7.20 Hz, PPh_3), 7.48 (d, 1H, $J_{H,H}$ = 7.98 Hz, Ar-H), 9.83 (s, 1H, —CH═N). ^{13}C NMR ($CDCl_3$, 100 MHz) δ (ppm): 17.94, 18.09, 18.91, 117.97, 121.52, 125.23, 127.86, 127.89, 128.02, 128.11, 128.14, 128.23, 128.64, 128.70, 129.80, 132.63, 133.45, 133.59, 133.81, 133.92, 135.53, 139.83, 149.34, 150.91, 151.38 and 218.80. ^{13}P NMR (121.50 MHZ, $CDCl_3$): δ = 6.95 IR υ (cm^{-1}): 2950 (w), 1634(s), 1477(s), 1092(s), 876(s), 426(m), 488(m). UV–Vis ($CHCl_3$, λ_{max}, nm), 289 and 335. Anal. calcd for $AgBrC_{52}H_{44}N_2P_2S_2$: C, 61.73; H, 4.48; N, 2.77; S, 6.34. Found: C, 62.43; H, 4.55; N, 2.84; S, 6.24.

*3.1.5. Synthesis of [Ag(PPh$_3$)$_2$L5] **5***

The reaction of **L5** (0.32 g, 7 mmol) and $[Ag(PPh_3)_2$**L5**] (0.30 g, 7 mmol) in acetonitrile furnished complex **5** as a yellow powder. Yield: (0.43 g, 70%). Melting point: 197–198 °C. ^1H NMR ($CDCl_3$, 400 MHz): δ (ppm) 2.26 (s, 6H, CH_3-Ar), 2.31 (s, 3H, CH_3-Ar), 6.93 (t, 1H, $J_{H,H}$ = 8.04 Hz, Ar-H), 6.97 (d, 3H, $J_{H,H}$ = 7.57 Hz, Ar-H), 7.22 (t, 1H, $J_{H,H}$ = 7.64 Hz, Ar-H), 7.28 (m, 12H, $J_{H,H}$ = 7.81 Hz, PPh_3), 7.39 (m, 18H, $J_{H,H}$ = 7.96 Hz, PPh_3), 9.87 (s, 1H, —CH═N). ^{13}C NMR ($CDCl_3$, 100 MHz) δ (ppm): 18.48, 128.09, 128.14, 128.20, 128.44, 129.17, 129.22, 129.30, 129.35, 130.32, 130.37, 130.42, 133.24, 133.29, 133.35, 133.40, 133.50, 133.56, 134.33,

134.37, 134.48, 134.53, 135.07, 135.16, 137.59, 150.55, 151.79, and 218.52. ^{13}P NMR (121.50 MHZ, $CDCl_3$): δ = 6.77. IR υ (cm^{-1}): 3051(w), 1623(s), 1478(s), 1093(s), 877(s), 420(m), 503(m). UV–Vis ($CHCl_3$, λ_{max}, nm), 290 and 335. Anal. calcd for $AgBrC_{53}H_{47}N_2P_2S_2$: C, 62.06; H, 4.62; N, 2.73; S, 6.25. Found: C, 62.50; H, 4.24; N, 2.70; S, 5.45.

3.1.6. Synthesis of [Cu(PPh$_3$)$_2$L1] 6

The reaction of **L1** (0.41 g, 1 mmol) and [Cu(PPh$_3$)$_2$**L1**] (0.65 g, 1 mmol) in acetonitrile furnished complex **6** as a yellow powder. Yield: (0.86 g, 81%). Melting point: 234–236 °C. ^{1}H NMR ($CDCl_3$, 400 MHz): δ (ppm) 2.23 (s, 6H, CH_3-Ar), 6.86 (t, 1H, $J_{H,H}$ = 8.06 Hz, Ar-H), 7.11 (d, 2H, $J_{H,H}$ = 7.35 Hz, Ar-H), 7.18 (t, 15H, $J_{H,H}$ = 7.84 Hz, PPh_3), 7.24 (t, 4H, $J_{H,H}$ = 7.67 Hz, PPh_3), 7.32 (d, 11*H*, $J_{H,H}$ = 7.81 Hz, PPh_3), 9.67 (s, 1H, —CH═N). ^{13}C NMR ($CDCl_3$, 100 MHz) δ (ppm): 17.88, 124.13, 127.35, 128.04, 128.09, 128.39, 128.56, 129.48, 133.67, 136.13, 152.33 and 215.30. ^{13}P NMR (121.50 MHZ, $CDCl_3$): δ = 0.1976 IR υ (cm^{-1}): 3053(w), 1632(s), 1477(s), 1027(s), 879(s), 495. UV–Vis ($CHCl_3$, λ_{max}, nm): 277 and 336. Anal. calcd for $C_{52}Cl_2CuH_{44}N_2P_2S_2$: C, 65.23; H, 4.63; N, 2.93; S, 6.70. Found: C, 65.35; H, 4.61; N, 2.83; S, 6.79.

3.1.7. Synthesis of [Cu(PPh$_3$)$_2$L2] 7

The reaction of **L2** (0.46 g, 1 mmol) and [Cu(PPh$_3$)$_2$**L2**] (0.65 g, 1 mmol) in acetonitrile furnished complex **7** as a yellow powder. Yield: (0.86 g, 77%). Melting point: 209–211 °C. ^{1}H NMR ($CDCl_3$, 400 MHz): δ (ppm) 0.97 (d, 6H, $J_{H,H}$ = 6.43 Hz, CH_3-CH), 1.23 (d, 6H, $J_{H,H}$ = 6.92 Hz, CH_3-CH), 2.89 (m, 2H, $J_{H,H}$ = 6.60 Hz, CH-CH_3), 6.86 (t, 1H, 8.02 Hz, Ar-H), 7.18 (m, 15H, $J_{H,H}$ = 7.77 Hz, PPh_3), 7.29 (m, 15H, $J_{H,H}$ = 7.87 Hz, PPh_3), 7.32 (d, 4H, $J_{H,H}$ = 8.09 Hz, Ar-H), 7.37 (t, 1H, $J_{H,H}$ = 7.56 Hz, PPh_3), 10.02 (s, 1H, —CH═N). ^{13}C NMR ($CDCl_3$, 100 MHz) δ (ppm): 24.60, 24.72, 28.75, 124.03, 124.08, 127.47, 128.29, 128.38, 129.22, 129.45, 133.67, 133.96, 134.32, 145.95, 146.21, 154.47 and 218.04. ^{13}P NMR (121.50 MHZ, $CDCl_3$): δ = −0.2015. IR υ (cm^{-1}): 2963(w), 1632(s), 1479(s), 1025 (s), 880(s), 490. UV–Vis ($CHCl_3$, λ_{max}, nm): 275 and 334. Anal. calcd for $C_{56}Cl_2CuH_{52}N_2P_2S_2$: C, 66.36; H, 5.17; N, 2.76; S, 6.33. Found: C, 66.31; H, 4.98; N, 2.64; S, 6.51.

3.1.8. Synthesis of [Cu(PPh$_3$)$_2$L3] 8

The reaction of **L3** (0.30 g, 1 mmol) and [Cu(PPh$_3$)$_2$**L3**] (0.65 g, 1 mmol) in acetonitrile furnished complex **8** as a yellow powder. Yield: (0.68 g, 72%). Melting point: 211–213 °C. ^{1}H NMR ($CDCl_3$, 400 MHz): δ (ppm) 2.19 (s, 6H, CH_3-Ar), 2.27 (s, 3H, CH_3-Ar), 6.85 (t, 1H, $J_{H,H}$ = 7.93 Hz, Ar-H), 6.93 (s, 2H, Ar-H), 7.17 (t, 12H, $J_{H,H}$ = 8.00 Hz, PPh_3), 7.24 (t, 3H, $J_{H,H}$ = 7.88 Hz, PPh_3), 7.30 (t, 15H, $J_{H,H}$ = 7.76 Hz, PPh_3), 9.69 (s, 1H, —CH═N). ^{13}C NMR ($CDCl_3$, 100 MHz) δ (ppm): 17.81, 18.82, 20.71, 21.35, 124.09, 127.39, 128.01, 128.38, 128.50, 129.07, 129.47, 133.68, 133.94, 135.14, 135.33, 135.66, 137.78, 138.01, 145.82, 152.43 and 216.58. ^{13}P NMR (121.50 MHZ, $CDCl_3$): δ = 0.2015. IR υ (cm^{-1}): 3047(w), 1633(s), 1479(s), 1027(s), 881(s), 490 (s). UV–Vis ($CHCl_3$, λ_{max}, nm): 274 and 335. Anal. calcd for $C_{53}Cl_2CuH_{46}N_2P_2S_2$: C, 65.53; H, 4.77; N, 2.88; S, 6.60. Found: C, 65.41; H, 4.78; N, 2.75; S, 6.52.

3.1.9. Synthesis of [Cu(PPh$_3$)$_2$L4] 9

The reaction of **L4** (0.42 g, 1 mmol) and [Cu(PPh$_3$)$_2$**L4**] (0.65 g, 1 mmol) in acetonitrile furnished complex **9** as a yellow powder. Yield: (0.80 g, 75%). Melting point: 196–198 °C. ^{1}H NMR ($CDCl_3$, 400 MHz): δ (ppm) 2.20 (s, 6H, CH_3-Ar), 6.83 (t, 1H, $J_{H,H}$ = 7.28 Hz, Ar-H), 6.93 (m, 2H, $J_{H,H}$ = 7.36 Hz, Ar-H), 7.11 (d, 2H, $J_{H,H}$ = 7.08 Hz, Ar-H), 7.18 (t, 15H, $J_{H,H}$ = 7.24 Hz, PPh_3), 7.25 (s, 1H, Ar-H), 7.30 (d, 15H, $J_{H,H}$ = 7.24 Hz, PPh_3), 7.48 (d, 1H, $J_{H,H}$ = 7.88 Hz, Ar-H), 9.53 (s, 1H, —CH═N). ^{13}C NMR ($CDCl_3$, 100 MHz) δ (ppm): 17.89, 18.04, 18.87, 117.91, 121.52, 123.10, 125.29, 127.89, 127.91, 128.04, 128.11, 128.21, 128.38, 129.46, 132.68, 132.88, 133.68, 133.96, 135.79, 138.37, 149.26, 149.37, 149.86 and 216.09. ^{13}P NMR (121.50 MHZ, $CDCl_3$): δ = −0.0078 IR υ (cm^{-1}): 3051(w), 1616(s), 1465(s), 1024(s), 874(s), 495(s). UV–Vis ($CHCl_3$, λ_{max}, nm): 274 and 333. Anal. calcd for $BrC_{52}CuH_{45}N_2P_2S_2$: C, 64.56; H, 4.69; N, 2.90; S, 6.63. Found: C, 64.88; H, 4.82; N, 2.71; S, 6.77.

3.1.10. Synthesis of [Cu(PPh$_3$)$_2$L5] 10

The reaction of **L5** (0.30 g, 1 mmol) and [Cu(PPh$_3$)$_2$**L5**] (0.65 g, 1 mmol) in acetonitrile furnished complex **10** as a yellow powder. Yield: (0.67 g, 70%). Melting point: 202–204 °C. ^{1}H NMR ($CDCl_3$, 400 MHz): δ (ppm) 2.16 (s, 6H, CH_3-Ar), 2.27 (s, 3H, CH_3-Ar), 6.90 (m, 4H, $J_{H,H}$ = 7.20 Hz, Ar-H), 7.17 (t, 14H, $J_{H,H}$ = 7.52 Hz, PPh_3), 7.25 (s, 1H, Ar-H), 7.30 (m, 16H, $J_{H,H}$ = 7.52 Hz, PPh_3), 7.48 (d, 1H, $J_{H,H}$ = 7.92 Hz, Ar-H), 9.67 (s, 1H, —CH═N). ^{13}C NMR ($CDCl_3$, 100 MHz) δ (ppm): 17.81, 17.97, 18.81, 117.79, 121.68, 125.21, 127.87, 128.00, 128.38, 128.99, 129.46, 132.63, 133.68, 133.98, 135.33, 135.67, 137.91, 149.47, 149.59, 216.22. ^{13}P NMR (121.50 MHZ, $CDCl_3$): δ = −0.0899 IR υ (cm^{-1}): 3053(w), 1625(s), 1479(s), 1025(s), 881(s), 492(s). UV–Vis ($CHCl_3$, λ_{max}, nm), 274 and 337. Anal. calcd for $BrC_{53}CuH_{47}N_2P_2S_2$: C, 64.86; H, 4.83; N, 2.85; S, 6.53. Found: C, 64.46; H, 4.63; N, 2.72; S, 6.81.

3.2. Single-crystal X-ray diffraction

Crystal evaluation and data collection of **1**–**3** and **6**–**10** were done on a Bruker Smart APEXII diffractometer with Mo Kα radiation (I = 0.71073 Å) equipped with an Oxford Cryostream low-temperature apparatus operating at 100 K for all samples. Reflections were collected at different starting angles and the *APEXII* program suite was used to index the reflections (Bruker, 2000a). Data reduction was performed using the *SAINT* (Bruker, 2009c) software and the scaling and absorption corrections were applied using the *SADABS* (Bruker, 2009b) multi-scan technique. The structures were solved by the direct method using the *SHELXS* program and refined using *SHELXL* program (Sheldrick, 2008). Graphics of the crystal structures were drawn using Mercury software (Macrae et al., 2008). Non-hydrogen atoms were first refined isotropically and then by anisotropic refinement with the full-matrix least square method based on F^2 using *SHELXL*. All hydrogen atoms were positioned geometrically, allowed to ride on their parent atoms and refined isotropically. The crystallographic data and structure refinement parameters for complex **1**, **3, 5, 6**, **8**, **9** and **10** are given in Tables 1 and 2. For complex **3**, a solvents mask was calculated and 56.0 electrons were found to exist in a void with a volume of

Table 1 The summary of X-ray crystal data collection and structure refinement parameters for complex **1**, **3**, **5** and **6.**

	1	**3**	**5**	**6**
Empirical formula	$C_{52}H_{43}AgCl_2N_2P_2S_2$	$C_{53}H_{45}AgCl_2N_2P_2S_2$	$C_{54}H_{48}AgBrCl_2N_2P_2S_2$	$C_{53}H_{45}Cl_4CuN_2P_2S_2$
Formula weight	1000.71	1014.74	1109.68	1041.31
Crystal system	Triclinic	monoclinic	Triclinic	triclinic
Space group	*P*-1	P 21/c	*P*-1	*P* −1
a/Å	9.6553(2)	16.7027(7)	10.5382(3)	12.2942(6)
b/Å	12.9062(2)	12.8700(5)	14.7215(4)	15.2958(7)
c/Å	19.1533(3)	24.2294(10)	17.1591(5)	15.3366(7)
α/°	92.3760°	90	81.1460(10)	106.825(2)
β/°	91.7670(10)°.	90.3260(10)	74.3610(10)	108.178(2)
γ/°	103.5790(10)°	90	75.7040(10)	101.797(2)
Volume/Å^3	2316.02(10)	5208.4(4)	2473.19(12)	2481.2(2)
Z	2	4	2	2
ρ_{calc}g/cm^3	1.435	1.298	1.490	1.394
μ/mm^{-1}	0.748	1.107	1.511	0.843
F(000)	1024	2080	1128	1072
Crystal size/mm^3	0.43 × 0.34 × 0.12	0.32 × 0.23 × 0.21	0.29 × 0.21 × 0.12	0.26 × 0.24 × 0.14
2Θ range for data collection/°	1.104 to 28.382°	2.309 to 33.347	1.804 to 28.324	1.66 to 28.24
Index ranges	$-29 \le h \le 29$ $-12 \le k \le 12$ $-30 \le l \le 30$	$-22 \le h \le 19$ $-18 \le k \le 16$ $-32 \le l \le 26$	$-14 \le h \le 14$ $-19 \le k \le 19$ $-22 \le l \le 22$	$-16 \le h \le 15$ $-20 \le k \le 20$ $-19 \le l \le 15$
Reflections collected	29,023	24,816	39,857	29,938
Independent reflections	10,883 [R_{int} = 0.0123]	13,053 [R_{int} = 0.0398]	12,155 [R_{int} = 0.0148]	11,724 [R_{int} = 0.0279]
Data/restraints/parameters	10883/2/550	1305/0/595	12155/0/577	11724/0/577
Goodness-of-fit on F^2	1.058	1.041	0.975	1.011
Final R indexes [I ≥ 2σ (I)]	R_1 = 0.0325, wR_2 = 0.0895	R_1 = 0.0312, wR_2 = 0.0739	R_1 = 0.0225, wR_2 = 0.0587	R_1 = 0.0430, wR_2 = 0.01171
Final R indexes [all data]	R_1 = 0.0342, wR_2 = 0.0909	R_1 = 0.0439, wR_2 = 0.0675	R_1 = 0.0225, wR_2 = 0.0610	R_1 = 0.0538, wR_2 = 0.01242
Largest diff. peak and hole (e Å^{-3})	0.733 and −1.526	0.635 and −0.621	0.623 and −0.0610	0.785 and −1.260

188.0 Å^3 which is consistent with the presence of 1.333 dichloromethane molecules per asymmetric unit. The solvent was highly disordered and attempts to model them were led to unstable refinement and were omitted using the *SQUEEZE* option (Spek, 2015) in *PLATON* (Spek, 2009). In the structure of complex **9**, the 2-bromophenyl substituent is disordered over three positions with specific site occupancies for each atom of this molecule while in complex **10**, the bromine atom is disordered over two positions with a major component having 94% site occupancy.

3.3. In vitro antimicrobial studies

The antimicrobial studies of the heteroleptic Ag(I) and Cu(I) dithiocarbamate PPh_3 metal complexes were performed using Clinical and Laboratory Standard Institute (CSLI) guidelines with slight modification (Wayne, 2018). They were evaluated against four gram-negative bacteria, viz: *Salmonella typhimurium* ATCC 14026, *Pseudomonas aeruginosa* ATCC 27853, *Escherichia coli* ATCC 25922 and *Klebsiella pneumoniae* ATCC 31488 and two gram-positive bacteria, viz: *Staphylococcus aureus* ATCC 700699 (methicillin-resistant) and *Staphylococcus aureus* ATCC 25923. Ciprofloxacin was used as a standard antibiotic for comparison while DMSO was used as a negative control and it showed no antibacterial activity against any of the bacterial strains used for this study at different concentrations. The samples were prepared by dissolving 1000 μg of the test sample in 1 ml of dimethyl sulfoxide (DMSO). The bacteria were inoculated onto Nutrient Agar (Biolab, South Africa) plates using the streak plate technique and incubated at 37 °C for 18 h (Govender et al., 2018). A single colony was isolated and inoculated into 10 ml sterile Nutrient Broth (Biolab, South Africa). This was incubated at 37 °C for 18 hr in a shaking incubator (100 rpm). The concentration of each bacterial strain was adjusted with sterile distilled water to achieve a final concentration equivalent to 0.5 Mc Farland's Standard (i.e. 1.5×10^8 cfu/mL) using a densitometer (Mc Farland Latvia) (Aremu et al., 2017). Thereafter, the Muller-Hilton Agar (MHA) plates were lawn inoculated with the diluted bacteria using a sterile throat swab. 5 μL of each sample was spotted onto the MHA plates and the plates were incubated at 37 °C for 18 h and then assessed for antibacterial activity which was denoted by a clear zone at the point of spotting. Samples that showed antimicrobial potential during antibacterial screening were tested further to determine their minimum inhibitory concentration (MICs). The samples were serially diluted 10 times to achieve concentrations ranging from 1000 μg/ml to 0.2 μg/ml. For the samples where MICs were lower than 0.2 μg/mL, the solutions were further diluted serially 5 times to achieve concentrations ranging from 0.100 μg/ml to 0.00625 μg/ml. 5 μL of each sample at different concentrations was spotted onto the MHA plates and the plates were incubated at 37 °C for 18 h and then assessed for their MIC. These were done in triplicate to ensure reproducibility

Table 2 The summary of X-ray crystal data collection and structure refinement parameters for complex **8**, **9** and **10.**

	8	**9**	**10**
Empirical formula	$C_{53}H_{45}Cl_2CuN_2P_2S_2$	$C_{52}H_{44}BrCuN_2P_2S_2$	$C_{54}H_{48}BrCl_2CuN_2P_2S_2$
Formula weight	970.41	946.72	1065.35
Crystal system	triclinic	monoclinic	Triclinic
Space group	$P\ -1$	P 21/n	$P\ -1$
a/Å	12.4084(2)	22.4506(7)	12.3468(2)
b/Å	13.3139(2)	9.6562(3)	13.0249(20
c/Å	16.01132(2)	22.6611(7)	17.8668(3)
α/°	83.3890(10)	90	73.4720(10)
β/°	81.1170(10)	108.8560(10)	87.1780(10)
γ/°	65.0040(10)	90	63.7040(10)
Volume/Å^3	2364.95(6)	4649.0(3)	2458.62(7)
Z	2	2	2
ρ_{calc}g/cm^3	1.363	1.353	1.438
μ/mm^{-1}	0.769	1.319	1.554
F(000)	1004	1948	1.092
Crystal size/mm^3	0.36 × 0.21 × 0.12	0.33 × 0.24 × 0.15	0.34 × 0.220 × 0.170
2Θ range for data collection/°	1.823 to 28.524	1.899 to 28.390	1.824 to 28.474
Index ranges	$-16 \le h \le 13$ $-17 \le k \le 17$ $-21 \le l \le 21$	$-29 \le h \le 29$ $-6 \le k \le 12$ $-30 \le l \le 30$	$-16 \le h \le 16$ $-16 \le k \le 17$ $-23 \le l \le 23$
Reflections collected	27,947	52,335	37,035
Independent reflections	11,783 [R_{int} = 0.0279]	11,617 [R_{int} = 0.0299]	12,146 [R_{int} = 0.0187]
Data/restraints/parameters	11783/0/559	11617/232/615	12146/0/587
Goodness-of-fit on F^2	0.962	1.074	0.950
Final R indexes [$I \ge 2\sigma$ (I)]	R_1 = 0.0403, wR_2 = 0.0883	R_1 = 0.0425, wR_2 = 0.0910	R_1 = 0.0379, wR_2 = 0.0922
Final R indexes [all data]	R_1 = 0.0636, wR_2 = 0.0978	R_1 = 0.0589, wR_2 = 0.0971	R_1 = 0.0479, wR_2 = 0.0978
Largest diff. peak and hole (e Å^{-3})	0.531 and −0.481	1.117 and −1.305	0.968 and −1.430

and the MIC was determined as the lowest concentration of the compounds at which no visible bacterial growth was observed after incubation.

3.4. DPPH free radical scavenging activity

The free radical-scavenging activity of complexes **1**–**10** was measured in terms of hydrogen donating or radical scavenging ability using the stable radical, DPPH as described by Chandrika *et al* with slight modifications (Liyana-Pathirana and Shahidi, 2005). Briefly, stock solutions (100 μL) of varying concentrations (1.0 mM, 0.75 mM, 0.50 mM, and 0.25 mM) of the test sample was added to an equal quantity of 0.1 mM solution of DPPH in ethanol. The reaction mixture was vortexed carefully and left in the dark at room temperature for 30 min. After 30 min of incubation at room temperature, the DPPH reduction was measured by reading the absorbance at 517 nm. Ascorbic acid of varying concentrations (1.0 mM, 0.75 mM, 0.50 mM, and 0.25 mM) was used as the reference compound. The ability of the compounds to scavenge DPPH radical was calculated as:

$$\%\ Scavenging\ \ Activity = \frac{Absorbance\ \ control - Absorbance\ \ of\ \ sample \times 100}{Absorbance\ \ control}$$

3.5. Nitric oxide radical inhibition assay

Nitric oxide is normally classified as a free radical because of its unpaired electron and reacts with oxygen or reactive oxygen species. It also displays important reactivity with certain types of proteins and other free radicals such as superoxide. NO is spontaneously produced by sodium nitroprusside solution at physiological pH 7.2, a fact that we take advantage of in this experiment. Under aerobic conditions, NO could interact with oxygen to produce stable nitrite ions quantifiable using Griess reagent. Compounds that scavenge NO radical, compete with oxygen thereby reducing the generation of nitrite ions (Pari and Saravanan, 2004).

We prepared the assay by incubating 100 μL of 10 mM sodium nitroprusside in a sodium phosphate buffer with pH of 7.4 and 100 μL of compounds **1** to **10** at different concentrations of the samples (0.25 mM, 0.50 mM, 0.75 mM and 1.0 Mm) at 37 °C for 2 h. Control samples without compounds **1**–**10** but with an equal volume of buffer were prepared in a similar manner as was done for the test samples. Thereafter, 100 μL of Griess reagent was added to the reaction mixture and transferred to 96-well plate and the absorbance measured at 546 nm (a chromophore is formed during the diazotization of the nitrite with Griess reagent). The percentage inhibition of NO generated by the test samples and the standard antioxidant ascorbic acid were calculated relative to the absorbance of the control.

$$\%\ Inhibition\ \ of\ \ NO = \frac{Absorbance\ \ control - Absorbance\ \ of\ \ sample \times 100}{Absorbance\ \ control}$$

4. Results and discussion

Complexes **1**–**10** were synthesized by treating an equimolar acetonitrile solution of potassium dithiocarbamate salt with a solution of bis(triphenylphosphine) silver(I)- or copper(I)-nitrate in dichloromethane at 25 °C (Scheme 1). All the complexes were obtained as air-stable pale-yellow solids in good

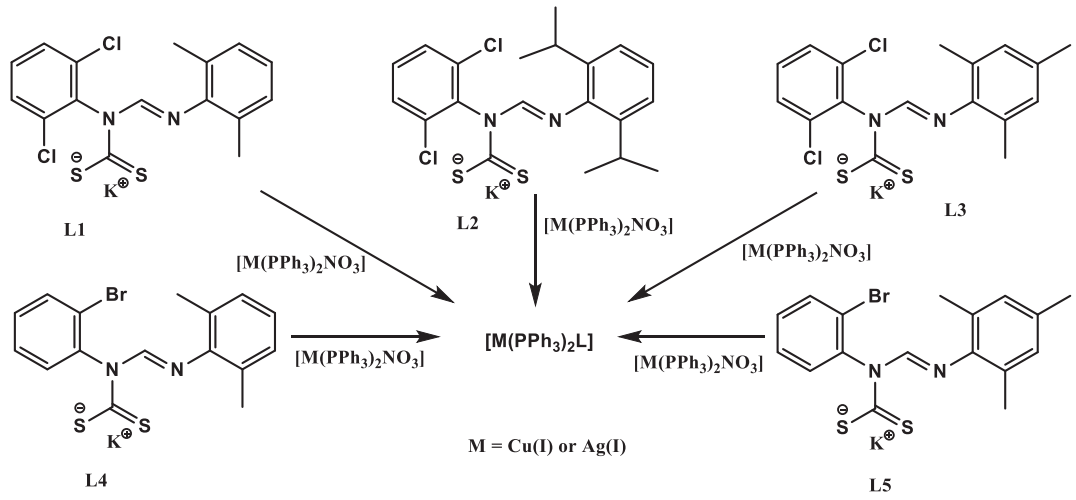

Scheme 1 Synthesis of heteroleptic Ag(I) and Cu(I) unsymmetrical N,N′-diarylformamidine dithiocarbamate PPh_3 complexes.

percentage yields of between 70 and 81. The Cu(I) complexes generally had higher melting points between 196 and 236 °C than the analogous Ag(I) complexes with melting points between 192 and 205 °C. All compounds were found to be soluble in polar solvents; dichloromethane, tetrahydrofuran, chloroform, dimethyl sulfoxide (DMSO) and N,N-dimethylformamide (DMF).

4.1. Spectroscopic studies

^{1}H and ^{13}C NMR spectra were all obtained in chloroform at 25 °C and were all in agreement with the formation of the Ag(I) and Cu(I) phosphine complexes **1**–**10**. The azomethine proton (NC*H* = N) was used to monitor the successful synthesis of all complexes. There was a general up-field shift from 10.07 to 10.39 ppm in the proton NMR spectra of the potassium formamidine dithiocarbamate salts, to 9.53–10.14 ppm in the proton spectra of complexes **1–10** confirming complexation (Table 3). The opposite was observed for the aliphatic protons where there was a general downfield shift, for example, the methyl protons in the spectrum of **L1** resonated as a singlet at 2.13 ppm but as singlets at 2.30 and 2.23 ppm upon complexation, as observed in the spectra of complexes **1** and **6**, respectively. This downfield shift can be attributed to the drift of the electron density towards the positive Ag(I) and Cu(I) centers in the complexes (Siddiqi et al., 2007; Mohammad et al., 2009) and the deshielding effect is more enhanced in the spectra of the Ag(I) complexes. The upfield shift for the signals associated with the -NCS_2 carbon in the ^{13}C NMR spectra of the complexes further confirmed complexation. In addition, singlets in each of the ^{31}P NMR spectra of at between 6.77 and 7.04 ppm in **1**–**5** and between −0.85 to 0.20 ppm for **6–10**, indicated the formation of the complexes and their purity (Rajput et al., 2012; Gupta et al., 2014; Mothes et al., 2015).

The C—NCS_2, C—S, and the Metal—S stretching modes of complexes **1–10** characteristic of dithiocarbamate salts complexes (Ahmad et al., 2006; Dimiza et al., 2010; Nazarov and Dyson, 2011; Nomiya et al., 2004), and υ(C═Nstr) of the azomethine (C(H)═N) (Gölcü, 2006; Gupta et al., 2014; Heard, 2005; Hogarth, 2012) were observed in their IR spectra. The thiouride stretching bands in the spectra of complexes **1–10** were observed between 1468 and 1479 cm^{-1} while those of dithiocarbamate ligands appeared between 1430 and 1477 cm^{-1}. The shift to higher wavenumbers in the complexes could be due to a mesomeric drift of electrons from the dithiocarbamate moiety towards the metal center (Moloto et al., 2009) and is indicative of the potassium salts η^2- symmetrical coordination to the metal center. In this form of coordination, the thiouride moiety boasts a partial double bond character confirmed by a single υ(C—S) band between 1024 and

Table 3 ^{1}H NMR and ^{13}C NMR chemical shifts for NC*H*═N and —NCS_2 in the spectra of **L1**–**L5** and **1**–**10** along with the IR bands for the thiouride C—N and the azomethine C═N_{str} for the ligands and complexes.

Ligands (Complex)	δ (—NCS_2) ppm	Δ δ	δ NC(H)═N ppm	Δ δ	υ(C═N) cm^{-1}	Δυ	υ(C—N) cm^{-1}	Δυ
DL1 (1)	218.82 (218.84)	0.02	10.12(9.86)	0.26	1614 (1640)	26	1432 (1477)	45
DL2 (2)	217.03 (220.58)	3.55	10.13(10.4)	0.01	1603 (1634)	31	1430 (1477)	47
DL3 (3)	219.04 (219.07)	0.03	10.39(9.86)	0.70	1612 (1639)	27	1435 (1479)	44
DL4 (4)	217.98 (218.80)	0.82	10.08(9.83)	0.25	1613 (1634)	21	1467 (1477)	10
DL5 (5)	219.43 (218.52)	0.91	10.07(9.87)	0.20	1614 (1623)	9	1465 (1478)	13
DL1 (6)	218.82 (215.30)	3.52	10.12(9.67)	0.45	1614 (1632)	18	1432 (1477)	45
DL2 (7)	217.03 (218.04)	1.01	10.13(10.0)	0.13	1603 (1632)	29	1430 (1479)	49
DL3 (8)	219.04 (216.58)	2.46	10.39(9.69)	0.70	1612 (1633)	21	1435 (1479)	44
DL4 (9)	217.98 (216.09)	1.89	10.08(9.53)	0.55	1613 (1616)	3	1467 (1468)	1
DL5 (10)	219.43 (216.22)	3.21	10.07(9.67)	0.40	1614 (1625)	11	1465 (1479)	14

1092 cm^{-1} for complexes **1**–**10** (Bonati and Ugo, 1967; Coucouvanis, 1970). The azomethine C═Nstr and the (C═N) bands were shifted to higher frequencies between 1616 and 1643 cm^{-1} in the complexes compared to those of the analogous salts which appear between 1603 and 1640 cm^{-1}. The Ag—P and Cu—P vibrational bands appear in the far-infrared region (between 418 and 445 cm^{-1} while those of Ag—S and Cu—S appear between 492 and 501 cm^{-1} for complexes **1** to **10**.

The UV–Visible spectra of complexes **1**–**10** in dichloromethane solution are given in Fig. 1a and b. The free dithiocarbamate ligands **L1** – **L5** exhibited two strong absorption bands in the UV region between 289 and 300 nm and, between 338 and 345 nm (Oladipo et al., 2019). The spectra of complexes **1**–**10** also have two strong absorption bands, but are blue shifted to between 272 and 292 and, 330 and 339 nm relative to those of **L1** to **L5**. The bands can be assigned to metal-perturbed $\pi \rightarrow \pi^*$ intraligand charged transfer transitions within dithiocarbamate and PPh_3 ligands (Rajput et al., 2012).

4.2. X-ray crystal structures analysis

Suitable crystals of **1**, **3**, **5**, **6**, **8**, **9** and **10** were each grown by slow evaporation of a dichloromethane/methanol solution. The molecular structures are presented in Figs. 2 and 3 while selected bond distances and angles are given in Table 4. The asymmetric units of each of the complexes **1**, **3**, **5**, **6**, **8**, **9** and **10** contain one whole molecule of the Ag(I) or Cu(I) dithiocarbamate phosphine complex and for complexes **5**, **6**, and **10**, also a molecule of dichloromethane solvent. In the molecular structures of the complexes, the metal center is coordinated to two S atoms from the dithiocarbamate ligand and two P atoms from the two triphenylphosphine ligands resulting in a distorted tetrahedral geometry. In this arrangement, the constrained bidentate S—C—S bite angle is much less than the ideal tetrahedral geometric angle (109°) and is between 66.93(2) ° and 75.12(2) °. This angle is evidently smaller in the Ag(I) complexes **1**, **3** and **5**. The P—M—P angles, on the other hand, are wider than 109°. However, the P—M—S angles are a lot closer to that of an ideal tetrahedral geometry with the lowest being 108° in **3** and the highest, 116° in **1** (Table 4). The constrained S—M—S angle and the bulkiness of phosphine ligands may be the cause for the deviation from ideal tetrahedral geometry. In all the complexes, the M—S, and M—P bond distances are shorter in the Cu complexes owing to, the greater force of attraction between electrons and, nuclei pull between Cu and S(P) relative to the one between Ag and S(P). In all complexes, the CS_2Ag chelate ring deviates from planarity with root mean square values being 0.0022, 0.0409, 0.0246, 0.0297, 0.0355, 0.0256 and 0.0213 Å for **1**, **3**, **5, 6**, **8**, **9,** and **10** respectively. All bond distances are comparable to those of similar compounds from the literature (Bianchini et al., 1985; Haiduc et al., 1995; Di Nicola et al., 2007; Mothes et al., 2015). The C—S bond lengths in all the complexes have a range 1.685(5)–1.702(5) Å and so are significantly shorter than the standard single C—S bond length of 1.81Å, due to π-electron delocalization over the $—NCS_2$ unit (Gupta et al., 2014) (see Table 5).

4.3. Antimicrobial activities evaluation

Complexes **1**–**10** were tested for antibacterial activity against *Klebsiella pneumoniae*, *Pseudomonas aeruginosa*, *Salmonella typhimurium*, *Escherichia coli*, methicillin-resistant *Staphylococcus aureus* (MRSA) and *Staphylococcus aureus*. Ciprofloxacin was used as a standard drug in the study. The minimum inhibitory concentration (MIC) values were used to evaluate the antimicrobial activities of the complexes and are summarized in Table 4 and higher MIC values are an indication of low antibacterial activity of the complexes (Lopez-Sandoval et al., 2008; Kumar et al., 2011; Mathews et al., 2019).

The 3D graphical representation of the MIC values in Fig. 4 show that complexes **1**–**5** had better antibacterial activity compared to the complexes **6**–**10**. Studies have shown that

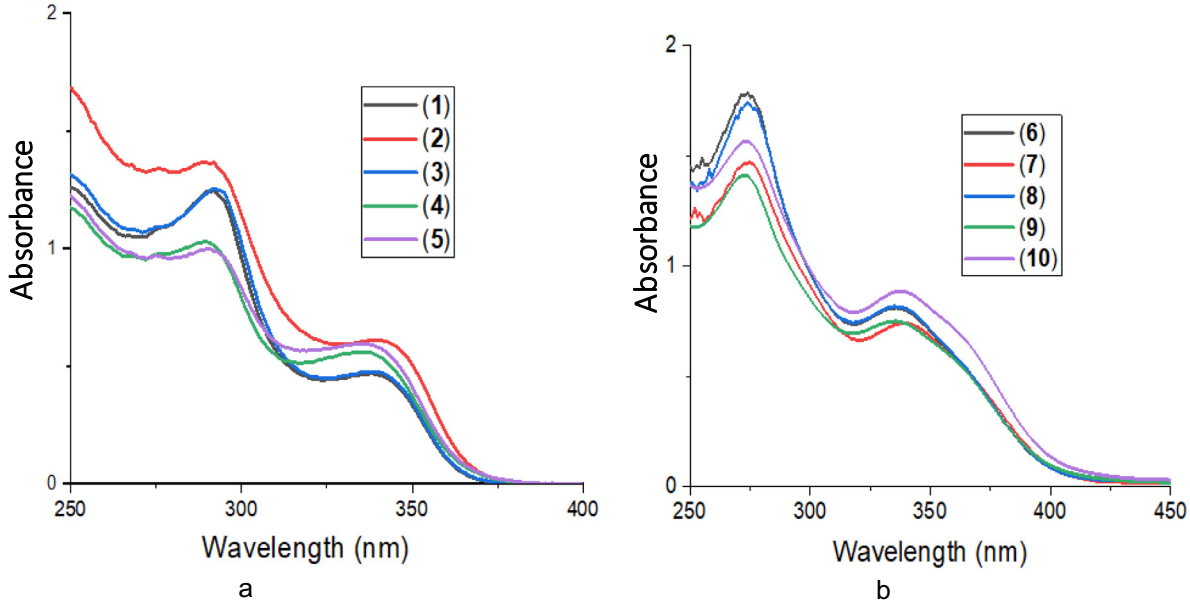

Fig. 1 (a) Electronic absorption spectra of **1**–**5** and (b) electronic absorption spectra of **6**–**10.**

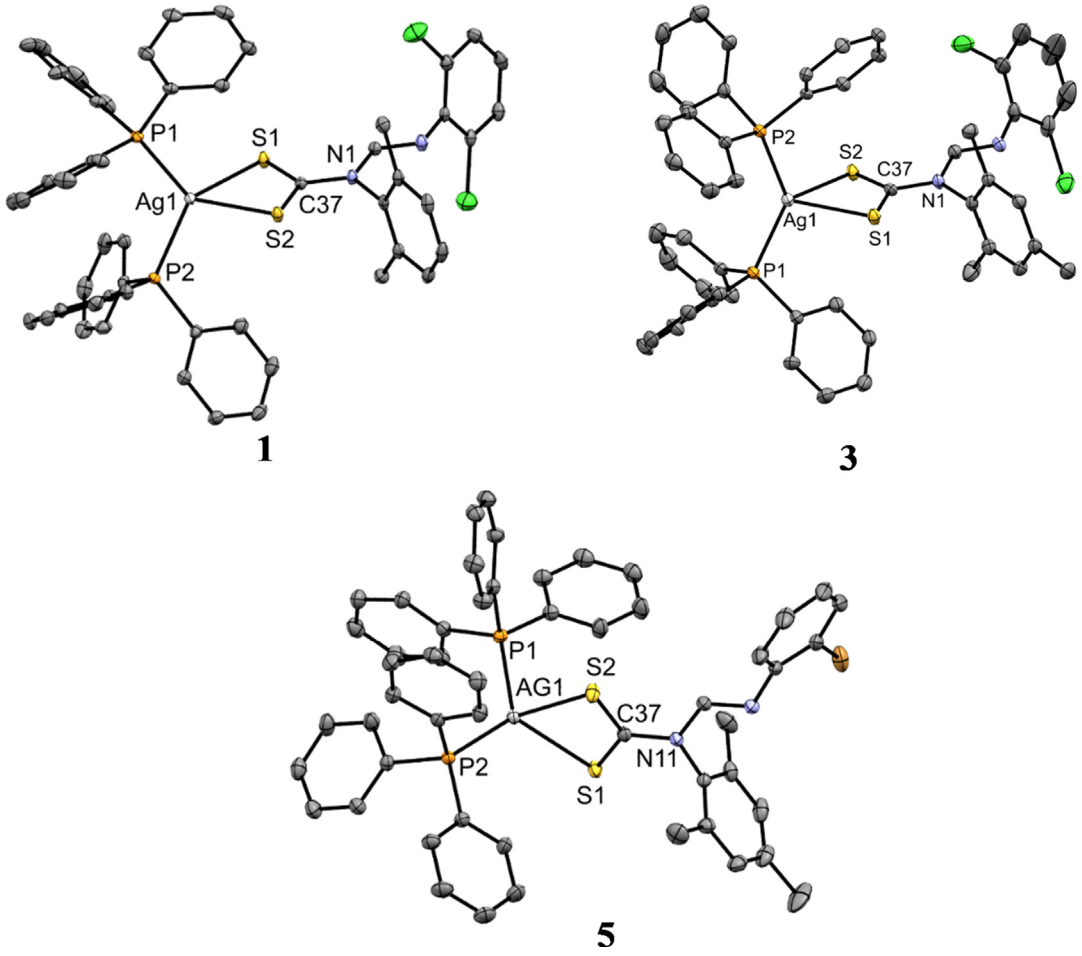

Fig. 2 ORTEP diagram of Ag(I) complexes **1**, **3**, and **5** drawn at 50% thermal ellipsoids probability. Hydrogen atoms have been omitted for clarity.

antimicrobial activity is very much dependent on the type of cell membranes of the bacteria by interacting with the lipids and proteins, and also, the nature of the metal ion electronic configuration (Guo and Sadler, 1999; Osowole et al., 2008; Mounika et al., 2010). The complexes have to penetrate the bacterial cell membranes to interact with the cytoplasm. Complexes **1** and **2** showed the most inhibitory effects against all strains except for *Salmonella typhimurium*. In fact, the effects against some of the strains was better than that of the standard, ciprofloxacin. For example, complexes **1** was twofold and **2** fourfold more potent than ciprofloxacin against *Pseudomonas aeruginosa*.

All Ag(I) complexes **1** to **5** displayed better activities against MRSA and *S. aureus* relative to ciprofloxacin while the opposite was observed for all Cu(I) complexes **6**–**10**. The MICs values for **1, 2**, and **3** were 3.125, 1.60 and 0.40 g/mL respectively compared to 25 ug/mL for ciprofloxacin against *S. aureus*. Complexes **3**, **4**, **5**, **9** and **10** only displayed moderate inhibitory activity against one or two strains with **10** being selectively active against *Salmonella typhimurium*. Complexes **6**, **7** and **8** were only active at high concentration (1000 ug/ml) against Gram-negative bacterial strains and completely inactive against Gram-positive bacterial strains.

In this study, the effect of metal center in the heteroleptic complexes on their activity against the bacteria was noticable. Complexes **1** to **5** were more active in comparison **6** to **10**. The Ag(I) ion has previously been reported to have the ability to change the bacteria cell wall's structure and cell constituents (Costal et al., 2012). The Ag ions are also known to bind effectively to the bacteria's DNA and RNA, thus preventing the bacteria from multiplying (Rai et al., 2009). On the other hand, the lower activity or lack of activity of **6** to **10** could (i), be as a results of either their inability to interact with membrane lipids and proteins hence inability to penetrate the bacterial cell walls or (ii) the posibility of **6** to **10** being modified and therefore rendered inactive as they penetrate the cell walls of the bacteria (Batzing, 2002). Structurally, higher electron presence as in diisopropyl groups seemed to result in better inhibitory activity. Comparatively, **2** with diisopropyl substituents performed better than **1** with methyl substituents on the phenyl rings of the complexes (Beniwal et al., 2017).

4.4. Antioxidant studies

4.4.1. DPPH radical scavenging assay

The ability of complexes to react with stable free radicals can be determined by DPPH assay. It has been reported that the strong absorption band at 517 nm in the UV–vis spectrum of DPPH results from the presence of an unpaired electron

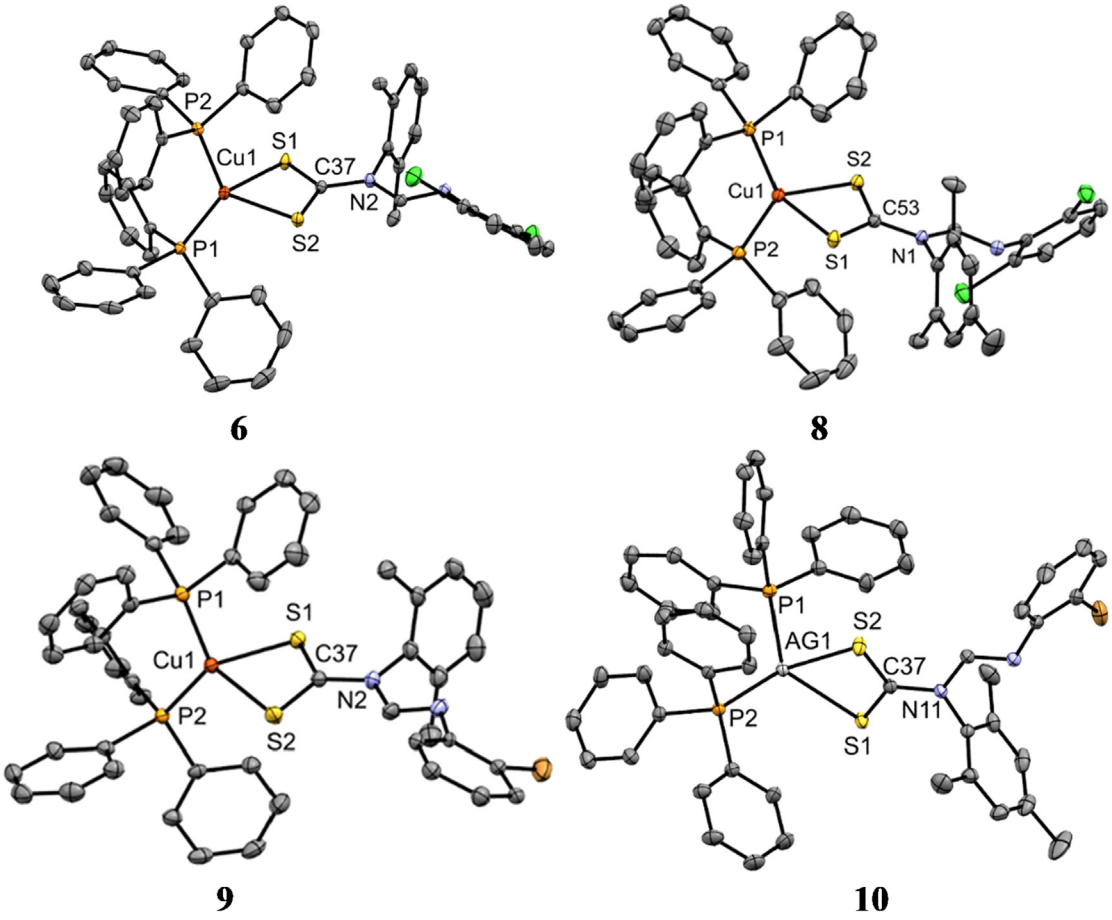

Fig. 3 ORTEP diagram of Ag(I) complexes **6**, **8**, **9** and **10** drawn at 50% thermal ellipsoids probability. Hydrogen atoms have been omitted for clarity.

Table 4 Selected bond length (Å) and angles (°) for complexes **1**, **3**, **5**, **6**, **8**, **9**, and **10** (M = Ag or Cu).

Parameters	**1**	**3**	**5**	**6**	**8**	**9**	**10**
Bond lengths							
M—P(1)	2.4511(7)	2.4561(7)	2.4735(5)	2.2307(5)	2.2353(5)	2.2475(7)	2.2427(8)
M—P(2)	2.4455(6)	2.4606(6)	2.4563(5)	2.2472(7)	2.2470(7)	2.2335(7)	2.2430(7)
M—S(1)	2.6670(6)	2.6589(6)	2.6490(5)	2.4181(7)	2.4194(7)	2.4215(7)	2.4177(5)
M—S(2)	2.6421(5)	2.7252(6)	2.6822(5)	2.3915(8)	2.3934(5)	2.3840(9)	2.3922(6)
C—S(1)	1.700(2)	1.683(2)	1.696(2)	1.692(3)	1.689(2)	1.694(3)	1.691(2)
C—S(2)	1.691(2)	1.703(2)	1.693(2)	1.697(3)	1.698(3)	1.696(3)	1.695(2)
C—N	1.394(2)	1.403(3)	1.398(2)	1.396(3)	1.393(3)	1.384(3)	1.392(2)
Bond angles							
P(1)—M—P(2)	118.883(2)	135.82(2)	123.06(2)	126.55(3)	129.91(3)	125.48(3)	127.78(3)
P(1)—M—S(1)	114.159(2)	108.37(2)	117.65(2)	112.60(2)	111.87(2)	105.39(3)	109.23(2)
P(1)—M—S(2)	116.556(2)	108.51(2)	100.49(2)	115.71(3)	112.34(2)	111.46(3)	112.89(2)
P(2)—M—S(1)	120.146(2)	107.86(2)	118.27(2)	103.59(2)	104.60(2)	115.57(3)	116.18(2)
P(2)—M—S(2)	108.333(2)	108.39(2)	109.41(2)	110.63(3)	109.37(2)	112.72(3)	102.79(2)
M—S(1)—C	84.75(7)	86.34(7)	85.39(5)	82.03(9)	82.08(8)	81.98(9)	82.27(9)
M—S(2)—C	85.73(7)	83.85(7)	84.37(5)	82.76(9)	82.70(8)	83.11(9)	82.95(9)
S(1)—C—S(2)	121.73(1)	122.5(1)	122.24(9)	119.80(1)	119.8(1)	119.3(3)	119.7(1)
S(1)—M—S(2)	67.81(2)	66.90(2)	67.65(1)	75.12(2)	75.03(2)	74.99(3)	74.99(2)

Table 5 Minimum inhibitory concentration of the metal complexes **1**–**10** (μg/mL).

Complexes	Gram (−) bacteria				Gram (+) bacteria	
	E. coli	*S. typhimurium*	*P. aeruginosa*	*K. pneumoniae*	*S. aureus*	MRSA
1	1.60	NA	0.40	0.80	3.125	0.40
2	0.40	NA	0.20	6.25	1.60	0.20
3	12.50	NA	6.25	12.50	0.40	0.20
4	0.40	NA	12.50	25.00	12.50	0.20
5	0.40	NA	NA	50.00	1.60	0.40
6	> 50	> 50	> 50	> 50	NA	NA
7	> 50	> 50	> 50	> 50	NA	NA
8	> 50	> 50	NA	NA	NA	NA
9	1.60	3.125	NA	NA	NA	NA
10	50	0.80	NA	NA	NA	NA
Ciprofloxacin[a]	0.20	0.40	0.80	1.60	25	25

NA = no activity and a = standard.

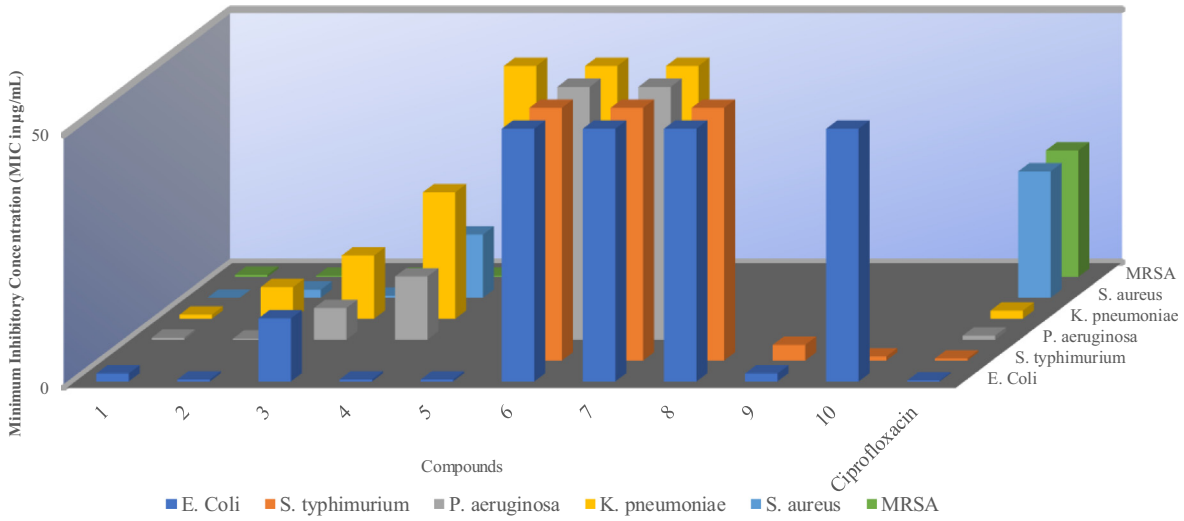

Fig. 4 Minimum inhibitory concentration (MIC) of the metal complexes vs bacteria cells. *The blank spaces represent no activity (NA) and 50 for MIC values of ≥ 50 μg/mL.

(Mahajan and Tandon, 2004; Dimiza et al., 2010; Vartale et al., 2016). This absorption band disappears when hydrogen or an electron from free radical scavengers pairs with this electron to form reduced DPPH, which leads to the abrupt change of DPPH colour from purple to yellow (Vartale et al., 2016). Compounds with DPPH scavenging ability are useful due to their anticancer, anti-aging, anti-inflammatory activities and for conditions such as rheumatoid arthritis (Kontogiorgis and Hadjipavlou-Litina, 2003; Vartale et al., 2016). In this study, we assessed the antioxidant activities of the complexes using IC_{50} values as calculated from their % free radical scavenging ability. Ascorbic acid (with an IC_{50} value of 1.01×10^{-3} mM) was used as a standard to evaluate the antioxidant property of the complexes (Table 6).

Complexes **1**, **2** and **3** had the least IC_{50} value of 1.60×10^{-3} mM, $1.34\ 10^{-3}$ mM and 1.90×10^{-3} mM respectively, but slightly higher than that of ascorbic acid and the highest value of ascorbic acid equivalent antioxidant capacity (AEAC), Complexes **6**, **8**, **9** and **10** displayed weak antioxidant activity. The electron-rich complexes showed better antioxidant activity than others (Oladipo et al., 2019). The Ag(I) complexes were found to display better DPPH radical scavenging ability than their Cu(I) complexes counter-part. Generally,

Table 6 Antioxidant potential of tested compounds **1**–**10** at different concentrations using DPPH and NO assay.

Complexes	DPPH Assay IC_{50} (mM)	NO Assay IC_{50} (mM)
1	1.60×10^{-3}	0.30
2	1.34×10^{-3}	0.25
3	1.90×10^{-3}	0.70
4	3.45×10^{-2}	1.20
5	4.56×10^{-2}	1.10
6	4.49×10^{-1}	> 10
7	2.45×10^{-2}	> 10
8	4.36×10^{-1}	> 10
9	7.59×10^{-1}	1.72
10	4.62×10^{-1}	1.21
Ascorbic acid	1.04×10^{-3}	0.23

the antioxidant activity of **1–10** increases as the concentration increases, which is illustrated in Fig. 5.

4.4.2. NO radical scavenging assay

The beneficial role of nitric oxide radical (NO·) as an important oxidative biological molecule in various physiological processes such as immune regulation, defense mechanism, blood pressure regulation, and neurotransmission have been reported (Archer, 1993; Beneš et al., 1999; Alderton et al., 2001). NO· is a reactive nitrogen species that contains one unpaired electron on the antibonding of $2\pi^*_y$ orbital (Beneš et al., 1999). The excess production of nitric oxide radical as well as other reactive nitrogen species is called nitrosative stress (Valko et al., 2006). This may lead to nitrosylation reactions, which alter protein structures and so have an adverse effect on body systems.

Compounds such as flavonoids (Vanacker et al., 1995), green tea (Nakagawa and Yokozawa, 2002), dithiocarbamates (Fujii and Yoshimura, 2000), and metal complexes (Fricker et al., 1997; Fujii and Yoshimura, 2000) have been reported to display good NO· scavenging ability. Herein, we study the ability of Ag(I) and Cu(I) dithiocarbamate-PPh_3 complexes, **1–10,** to scavenge NO·. The percentage nitric oxide radical scavenging activity values were used to calculate the IC_{50} of all the complexes and these are summarized in Table 6. When compared to the IC_{50} value of the standard, ascorbic acid, of 0.23 mM, compounds **1–10** exhibited moderate to good NO· scavenging ability with **1** and **2** better inhibitory activities, almost the same as that of ascorbic acid. Complexes **6**, **7**, and **8** displayed poor activity. The nitric oxide scavenging ability of **1–10** increases as the concentration increases and this is illustrated in Fig. 6.

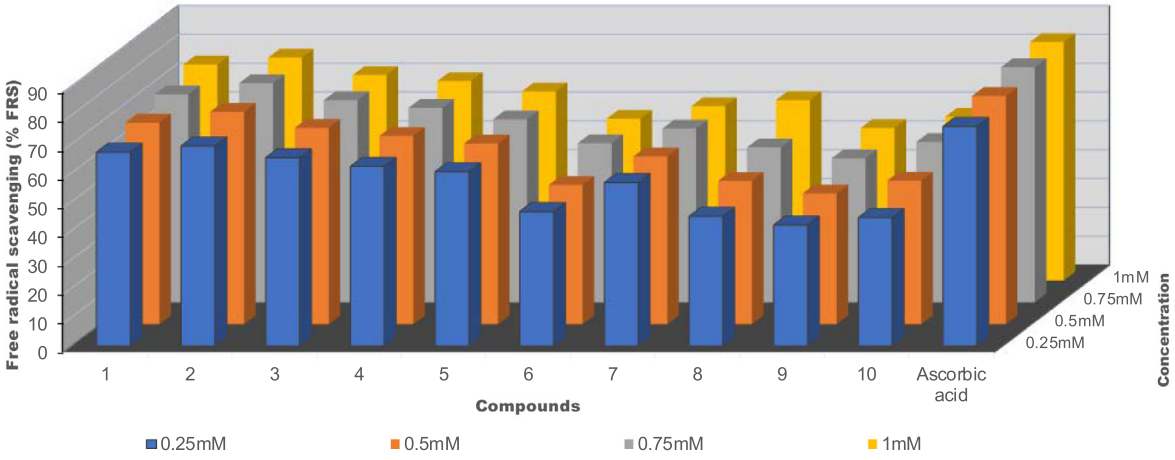

Fig. 5 **%** Free radical scavenging vs concentration (mM) of Ag(I) complexes **1–5** and Cu(I) complexes **6–10**.

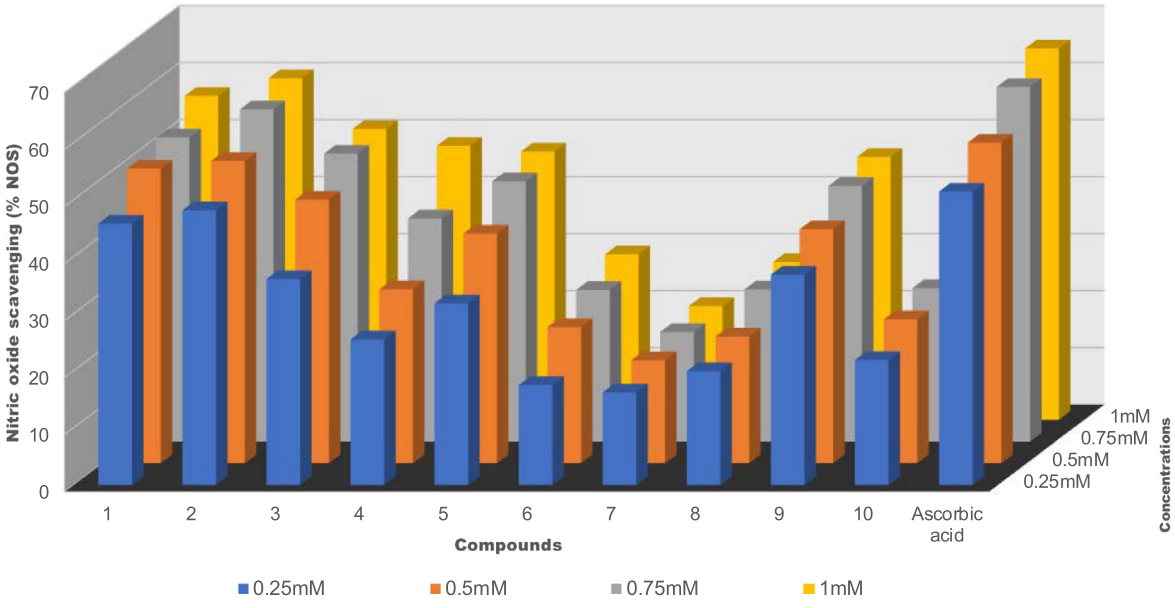

Fig. 6 % Nitric oxide scavenging vs concentration (mM) of Ag(I) complexes **1–5** and Cu(I) complexes **6–10.**

5. Conclusion

In conclusion, ten new heteroleptic silver(I) and copper(I) dithiocarbamate-PPh_3 complexes **1**–**10** have been synthesized and fully characterized by elemental analysis and spectroscopy techniques. Crystal structures of **1**, **3**, **5**, **6**, **8**, **9** and **10** showed that the geometry around the AgS_2P_2 and CuS_2P_2 core is distorted tetrahedral. The effect of metal center was highly noticeable as the complexes with Ag(I) exhibited better biological activity than Cu(I) couterpart. The MICs results showed that silver(I) complexes, **1**–**5** displayed better antimicrobial activity when compared to the copper(I) counterparts, **6**–**10** and even inhibited Gram-positive bacteria, MRSA around six times better than ciprofloxacin. In addition, electronics played a vital role in biological activity with complexes **1** and **2** showing better activity in all the studies. Complex **2** had the highest ascorbic acid equivalent capacity for both DPPH and NO assays.

6. Supplementary data

CCDC 1967730, CCDC 1967732, CCDC 1978699, CCDC 1967733, CCDC 1967735, CCDC 1967736 and CCDC 1967737 contain the supplementary crystallographic data for complexes **1**, **3, 5, 6, 8, 9** and **10** respectively. These data can be obtained free of charge via http://www.ccdc.cam.ac.uk/conts/retrieving.html, or from the Cambridge Crystallographic Data Centre, 12 Union Road, Cambridge CB2 1EZ, UK; fax: (+44)1223-336-033; or via e-mail: deposit@ccdc.cam.ac.uk.

Declaration of Competing Interest

The authors declare that they have no known competing financial interests or personal relationships that could have appeared to influence the work reported in this paper.

Acknowledgments

The authors would like to thank the College of Agriculture, Science, and Engineering, the University of Kwazulu-Natal and the National Research Foundation (NRF), South Africa for financial support.

References

Abramov, A., Forssberg, K., 2005. Chemistry and optimal conditions for copper minerals flotation: theory and practice. Min. Proc. Ext. Met. Rev. 26, 77–143.

Afzaal, M., Rosenberg, C.L., Malik, M.A., White, A.J., O'Brien, P., 2011. Phosphine stabilized copper(I) complexes of dithiocarbamates and xanthates and their decomposition pathways. New J. Chem. 35, 2773–2780.

Ahmad, S., Isab, A.A., Ali, S., Al-Arfaj, A.R., 2006. Perspectives in bioinorganic chemistry of some metal based therapeutic agents. Polyhedron 25, 1633–1645.

Alderton, W.K., Cooper, C.E., Knowles, R.G., 2001. Nitric oxide synthases: structure, function and inhibition. Biochem. J. 357, 593–615.

Archer, S., 1993. Measurement of nitric oxide in biological models. FASEB J. 7, 349–360.

Aremu, O.S., Gopaul, K., Kadam, P., Singh, M., Mocktar, C., Singh, P., Koorbanally, N.A., 2017. Synthesis, characterization, anti-cancer and antibacterial activity of some novel pyrano [2, 3-d] pyrimidinone carbonitrile derivatives. Anti-Cancer. Agent Me. 17, 719–725.

Barba, V., Arenaza, B., Guerrero, Reyes, J.R., 2012. Synthesis and structural characterization of diorganotin dithiocarbamates from 4-(ethylaminomethyl) pyridine. Heteroatom Chem. 23, 422–428.

Barreiro, E., Casas, J.S., Couce, M.D., Laguna, A., López-de-Luzuriaga, J.M., Monge, M., Sánchez, A., Sordo, J., López, E.M. V., 2013. A novel hexanuclear silver(I) cluster containing a regular Ag_6 ring with short Ag–Ag distances and an argentophilic interaction. Dalton Trans. 42, 5916–5923.

Batzing, B.L., 2002. Microbiology: An introduction. Wardsworth Group Brooks/Cole, pp. 61–64.

Beneš, L., Ďuračková, Z., Ferenčik, M., 1999. Chemistry, physiology and pathology of free radicals. Life Sci. 65, 1865–1874.

Beniwal, S., Chhimpa, S., Gaur, D., John, P., Singh, Y., Sharma, J., 2017. Syntheses, characterization, antibacterial activity and molecular modelling of phenylantimony(III) heteroleptic derivatives containing substituted oximes and piperidine. Appl. Organomet. Chem. 31, 3725.

Bera, P., Kim, C.H., Seok, C.I., 2010. Synthesis of nanocrystalline CdS from cadmium(II) complex of S-benzyl dithiocarbazate as a precursor. Solid State Sci. 12, 1741–1747.

Berners-Price, S.J., Johnson, R.K., Giovenella, A.J., Faucette, L.F., Mirabelli, C.K., Sadler, P.J., 1988. Antimicrobial and anticancer activity of tetrahedral, chelated, diphosphine silver(I) complexes: comparison with copper and gold. J. Inorg. Bio. 33, 285–295.

Bianchini, C., Ghilardi, C.A., Meli, A., Midollini, S., Orlandini, A., 1985. Reactivity of copper(I) tetrahydroborates toward carbon disulfide and phenyl isothiocyanate. Structures of (PPh3)2Cu (.mu.-S2CSCH2SCS2)Cu(PPh3)2,(PPh3)2Cu(S2COEt), and (PPh3)2Cu(S2CNHPh).CHCl3. Inorg. Chem. 24, 932–939.

Bonati, F., Ugo, R., 1967. Organotin (IV) n, n-disubstituted dithiocarbamates. J. Organo. Met. Chem. 10, 257–268.

Bruce, J.C., Revaprasadu, N., Koch, K.R., 2007. Cadmium(II) complexes of N, N-diethyl-N′-benzoylthio (seleno) urea as single-source precursors for the preparation of CdS and CdSe nanoparticles. New. J. Chem. 31, 1647–1653.

Bruker, 2009a. APEXII. Madison, Wisconsin, USA, APEXII Bruker AXS Inc.

Bruker, 2009b. SADABS. Madison, Wisconsin, USA, SADABS Bruker AXS Inc.

Bruker, 2009c. SAINT. Madison, Wisconsin, USA, SAINT Bruker AXS InC.

Cardell, D., Hogarth, G., Faulkner, S., 2006. A dithiocarbamate-stabilized copper(I) cube. Inorg. Chimi. Acta 359, 1321–1324.

Chisholm, M., Albert Cotton, F., Daniels, L., Huffman, J., Iyer, S., Macintosh, A., Murillo, C., 1999. Compounds in which the MO_2^{4+} unit is embraced by one, two or three formamidinate ligands together with acetonitrile ligands. Dalton Trans. 9, 1387–1392.

Clerac, R., Cotton, F.A., Dunbar, K.R., Murillo, C.A., Wang, X., 2001. Dinuclear and heteropolynuclear complexes containing MO_2^{4+} units. Inorg. Chem. 40, 420–426.

Costa, R.D., Tordera, D., Ortí, E., Bolink, H.J., Schönle, J., Graber, S., Housecroft, C.E., Constable, E.C., Zampese, J.A., 2011. Copper (I) complexes for sustainable light-emitting electrochemical cells. J. Mater. Chem. 21, 16108–16118.

Costal, G.S., Corbi, P.P., Abbehausen, C., Formiga, A.L., Lustri, W. R., Cuin, A., 2012. Silver(I) and gold(I) complexes with penicillamine: synthesis, spectroscopic characterization and biological studies. Polyhedron 34, 210–214.

Coucouvanis, D., 1970. The chemistry of the dithioacid and 1, 1-dithiolate complexes. Prog. Inorg. Chem. 11, 233–371.

Di Nicola, C., Ngoune, J., Pettinari, C., Skelton, B.W., White, A.H., 2007. Synthesis and structural characterization of adducts of silver (I) diethyldithiocarbamate with P-donor ligands. Inorg. Chim. Acta 360, 2935–2943.

Dimiza, F., Papadopoulos, A.N., Tangoulis, V., Psycharis, V., Raptopoulou, C.P., Kessissoglou, D.P., Psomas, G., 2010. Biological evaluation of non-steroidal anti-inflammatory drugs-cobalt(II) complexes. Dalton Trans. 39, 4517–4528.

Domaille, D.W., Zeng, L., Chang, C.J., 2010. Visualizing ascorbate-triggered release of labile copper within living cells using a ratiometric fluorescent sensor. J. Am. Chem. Soc. 132, 1194–1195.
Ekennia, A.C., Onwudiwe, D.C., Osowole, A.A., Olasunkanmi, L.O., Ebenso, E.E., 2016. Synthesis, biological, and quantum chemical studies of Zn(II) and Ni(II) mixed-ligand complexes derived from N, N-disubstituted dithiocarbamate and benzoic acid. J. Chem. 2016, 1–12.
El-Sherif, A.A., Jeragh, B.J., 2007. Mixed ligand complexes of Cu(II)-2-(2-pyridyl)-benzimidazole and aliphatic or aromatic dicarboxylic acids: synthesis, characterization and biological activity. Spectrochim. Acta. A 68, 877–882.
Elie, M., Sguerra, F., Di Meo, F., Weber, M.D., Marion, R., Grimault, A.L., Lohier, J.F.O., Stallivieri, A.L., Brosseau, A., Pansu, R.B., 2016. Designing NHC–copper(I) dipyridylamine complexes for blue light-emitting electrochemical cells. ACS Appl. Mater. Interfaces 8, 14678–14691.
Fereidoonnezhad, M., Niazi, M., Shahmohammadi Beni, M., Mohammadi, S., Faghih, Z., Faghih, Z., Shahsavari, H.R., 2017. Synthesis, biological evaluation, and molecular docking studies on the DNA binding interactions of platinum(II) rollover complexes containing phosphorus donor ligands. ChemMedChem 12, 456–465.
Ford, P.C., Cariati, E., Bourassa, J., 1999. Photoluminescence properties of multinuclear copper(I) compounds. Chem. Rev. 99, 3625–3648.
Frezza, M., Dou, Q.P., Xiao, Y., Samouei, H., Rashidi, M., Samari, F., Hemmateenejad, B., 2011. In vitro and in vivo antitumor activities and DNA binding mode of five coordinated cyclometalated organoplatinum(II) complexes containing biphosphine ligands. J. Med. Chem. 54, 6166–6176.
Fricker, S., Slade, E., Powell, N., Vaughan, O., Henderson, G., Murrer, B., Megson, I., Bisland, S., Flitney, F., 1997. Ruthenium complexes as nitric oxide scavengers: a potential therapeutic approach to nitric oxide-mediated diseases. Br. J. Pharmacol. 122, 1441–1449.
Fujii, S., Yoshimura, T., 2000. A new trend in iron–dithiocarbamate complexes: as an endogenous NO trapping agent. Coord. Chem. Rev. 198, 89–99.
Gölcü, A., 2006. Transition metal complexes of propranolol dithiocarbamate: synthesis, characterization, analytical properties and biological activity. Trans. Met. Chem. 31, 405–412.
Govender, H., Mocktar, C., Koorbanally, N.A., 2018. Synthesis and bioactivity of quinoline-3-carboxamide derivatives. J. Hetrocyl. Chem. 55, 1002–1009.
Guo, Z., Sadler, P.J., 1999. Metals in medicine. Angew. Chem. Int. Ed. 38, 1512–1531.
Gupta, A.N., Singh, V., Kumar, V., Prasad, L.B., Drew, M.G., Singh, N., 2014. Syntheses, crystal structures and optical properties of heteroleptic copper(I) dithio/PPh_3 complexes. Polyhedron 79, 324–329.
Güzel, Ö., Salman, A., 2006. Synthesis, antimycobacterial and antitumor activities of new (1, 1-dioxido-3-oxo-1, 2-benzisothiazol-2 (3H)-yl) methyl N, N-disubstituted dithiocarbamate/O-alkyldithiocarbonate derivatives. Bioorg. Med. Chem. 14, 7804–7815.
Gysling, H.J., Kubas, G.J., 1979. Coordination complexes of copper (I) nitrate. Inorg. Syntheses 19, 92–97.
Hadjikakou, S., Ozturk, I., Xanthopoulou, M., Zachariadis, P., Zartilas, S., Karkabounas, S., Hadjiliadis, N., 2008. Synthesis, structural characterization and biological study of new organotin (IV), silver(I) and antimony(III) complexes with thioamides. J. Inorg. Biochem. 102, 1007–1015.
Haiduc, I., Cea-Olivares, R., Toscano, R.A., Silvestru, C., 1995. X-ray crystal structure of (tetraphenyldithiomidodiphosphinato) (triphenylphosphine) copper(I),$(Ph_3P)Cu(SPPh_2)_2N$, a monocyclic inorganic (carbon-free) chelate ring compound. Polyhedron 14, 1067–1071.
Halimehjani, A.Z., Torabi, S., Amani, V., Notash, B., Saidi, M.R., 2015. Synthesis and characterization of metal dithiocarbamate derivatives of 3-((pyridin-2-yl) methylamino) propanenitrile: crystal structure of [3-((pyridin-2-yl) methylamino) propanenitrile dithiocarbamato] nickel(II). Polyhedron 102, 643–648.
Hanif, M., Saddiqa, A., Hasnain, S., Ahmad, S., Rabbani, G., Isab, A.A., 2008. Preparation, spectral characterization and antibacterial studies of silver(I) complexes of 2-mercaptopyridine and thiomalate. J. Spectrosc. 22, 51–56.
Heard, P.J., 2005. Main group dithiocarbamate complexes. Prog. Inorg. Chem. 53, 1–69.
Hogarth, G., 2012. Metal-dithiocarbamate complexes: chemistry and biological activity. Mini. Rev. Med. Chem. 12, 1202–1215.
Huang, C., Gou, S., Zhu, H., Huang, W., 2007. Cleavage of C−S bonds with the formation of a tetranuclear Cu(I) cluster. Inorg. Chem. 46, 5537–5543.
Isab, A.A., Wazeer, M.I., 2007. Synthesis and characterization of thiolate–Ag(I) complexes by solid-state and solution NMR and their antimicrobial activity. Spectrochim. Acta. A 66, 364–370.
Islam, S.I., Das, S.B., Chakrabarty, S., Hazra, S., Pandey, A., Patra, A., 2016. Synthesis, characterization, and biological activity of Nickel(II) and Palladium(II) complex with pyrrolidine dithiocarbamate (PDTC). Adv. Chem. 2016, 524–530.
Kamatchi, T.S., Chitrapriya, N., Lee, H., Fronczek, C.F., Fronczek, F.R., Natarajan, K., 2012. Ruthenium (II)/(III) complexes of 4-hydroxy-pyridine-2, 6-dicarboxylic acid with $PPh_3/AsPh_3$ as co-ligand: impact of oxidation state and co-ligands on anticancer activity in vitro. Dalton Trans. 41, 2066–2077.
Kontogiorgis, C., Hadjipavlou-Litina, D., 2003. Biological evaluation of several coumarin derivatives designed as possible anti-inflammatory/antioxidant agents. J. Enzym. Inhib. Med. Chem. 18, 63–69.
Kumar, L.S., Prasad, K.S., Revanasiddappa, H.D., 2011. Synthesis, characterization, antioxidant, antimicrobial, DNA binding and cleavage studies of mononuclear Cu(II) and Co(II) complexes of 3-hydroxy-N'-(2-hydroxybenzylidene)-2-naphthohydrazide. Eur. J. Chem. 2, 394–403.
Kumar, V., Singh, V., Gupta, A.N., Manar, K.K., Drew, M.G., Singh, N., 2014a. Influence of ligand environments on the structures and luminescence properties of homoleptic cadmium (II) pyridyl functionalized dithiocarbamates. CrystEngComm 16, 6765–6774.
Kumar, V., Singh, V., Gupta, A.N., Manar, K.K., Prasad, L.B., Drew, M.G., Singh, N., 2014b. Influence of ligand environment on the structure and properties of silver(I) dithiocarbamate cluster-based coordination polymers and dimers. New J. Chem. 38, 4478–4485.
Kutal, C., 1990. Spectroscopic and photochemical properties of d10 metal complexes. Coord. Chem. Rev. 99, 213–252.
Lim, M.H., Xu, D., Lippard, S.J., 2006. Visualization of nitric oxide in living cells by a copper-based fluorescent probe. Nat. Chem. Biol. 2, 375–380.
Liu, J., Shgenaga, M.K., Liang-Junyan, Y., Mori, A., Ames, B.N., 1996. Antioxidant activity of diethyldithiocarbamate. Free Radic. Res. 24, 461–472.
Liyana-Pathirana, C.M., Shahidi, F., 2005. Antioxidant activity of commercial soft and hard wheat (Triticum aestivum L.) as affected by gastric pH conditions. J. Arg. Food Chem. 53, 2433–2440.
Lopez-Sandoval, H., Londoño-Lemos, M.E., Garza-Velasco, R., Poblano-Meléndez, I., Granada-Macías, P., Gracia-Mora, I., Barba-Behrens, N., 2008. Synthesis, structure and biological activities of cobalt(II) and zinc(II) coordination compounds with 2-benzimidazole derivatives. J. Inorg. Biochem. 102, 1267–1276.
Macrae, C.F., Bruno, I.J., Chisholm, J.A., Edgington, P.R., McCabe, P., Pidcock, E., Rodriguez-Monge, L., Taylor, R., Van de Streek, J., Wood, P.A., 2008. Mercury CSD 2.0-new features for the visualization and investigation of crystal structures. Appl. Cryst. 41, 466–470.

Mahajan, A., Tandon, V.R., 2004. Antioxidants and rheumatoid arthritis. J. Indian Rheumatol Assoc. 12, 139–142.
Maji, S.K., Dutta, A.K., Dutta, S., Srivastava, D.N., Paul, P., Mondal, A., Adhikary, B., 2012. Single-source precursor approach for the preparation of CdS nanoparticles and their photocatalytic and intrinsic peroxidase like activity. Appl. Catal. B 126, 265–274.
Mathews, N.A., Jose, A., Kurup, M.P., 2019. Synthesis and characterization of a new aroylhydrazone ligand and its cobalt (III) complexes: X-ray crystallography and in vitro evaluation of antibacterial and antifungal activities. J. Mol. Struc. 1178, 544–553.
McKeage, M.J., Papathanasiou, P., Salem, G., Sjaarda, A., Swiegers, G.F., Waring, P., Wild, S.B., 1998. Antitumor activity of gold(I), silver(I) and copper(I) complexes containing chiral tertiary phosphines. Metal-Based Drug 5, 217–223.
Melekhova, A.A., Novikov, A.S., Panikorovskii, T.L., Bokach, N.A., Kukushkin, V.Y., 2017a. Novel family of homoleptic copper(I) complexes featuring disubstituted cyanamides: combined synthetic, structural, and theoretical study. New J. Chem. 41, 14557–14566.
Melekhova, A.A., Smirnov, A.S., Novikov, A.S., Panikorovskii, T. L., Bokach, N.A., Kukushkin, V.Y., 2017b. Copper(I)-catalyzed 1,3-dipolar cycloaddition of ketonitrones to dialkylcyanamides: a step towards sustainable generation of 2,3- dihydro-1,2,4-oxadiazoles. ACS Omega 2, 1380–1391.
Melekhova, A.A., Novikov, A.S., Luzyanin, K.V., Bokach, N.A., Starova, G.L., Gurzhiy, V.V., Kukushkin, V.Y., 2015. Tris-isocyanide copper(I) complexes: synthetic, structural, and theoretical study. Inorg. Chim. Acta 434, 31–36.
Mohamed, G.G., Ibrahim, N.A., Attia, H.A., 2009. Synthesis and anti-fungicidal activity of some transition metal complexes with benzimidazole dithiocarbamate ligand. Spectrochim. Acta 72, 610–615.
Mohammad, A., Varshney, C., Nami, S.A., 2009. Synthesis, characterization and antifungal activities of 3d-transition metal complexes of 1-acetylpiperazinyldithioc arbamate, M(acpdtc) 2. Spectrochim. Acta 73, 20–24.
Moloto, N., Revaprasadu, N., Moloto, M., O'Brien, P., Raftery, J., 2009. N, N'-diisopropylthiourea and N, N'-dicyclohexylthiourea zinc (II) complexes as precursors for the synthesis of ZnS nanoparticles. S. Afr. J. Sci. 105, 258–263.
Mothes, R., Petzold, H., Jakob, A., Rüffer, T., Lang, H., 2015. Dithiocarbamate copper(I) and silver(I) complexes: synthesis, structure and thermal behavior. Inorg. Chim. Acta 429, 227–236.
Mounika, K., Pragathi, A., Gyanakumari, C., 2010. Synthesis characterization and biological activity of a Schiff base derived from 3-ethoxy salicylaldehyde and 2-amino benzoic acid and its transition metal complexes. J. Sci. Res. 2, 513.
Mthethwa, T., Pullabhotla, V.R., Mdluli, P.S., Wesley-Smith, J., Revaprasadu, N., 2009. Synthesis of hexadecylamine capped CdS nanoparticles using heterocyclic cadmium dithiocarbamates as single source precursors. Polyhedron 28, 2977–2982.
Nakagawa, T., Yokozawa, T., 2002. Direct scavenging of nitric oxide and superoxide by green tea. Food Chem. Toxicol. 40, 1745–1750.
Nazarov, A.A., Dyson, P.J., 2011. Metal Phosphorus Complexes as Antitumor Agents. Phosphorus Compounds. Springer, pp. 445–461.
Nomiya, K., Yoshizawa, A., Tsukagoshi, K., Kasuga, N.C., Hirakawa, S., Watanabe, J., 2004. Synthesis and structural characterization of silver(I), aluminium(III) and cobalt(II) complexes with 4-isopropyltropolone (hinokitiol) showing noteworthy biological activities. Action of silver (I)-oxygen bonding complexes on the antimicrobial activities. J. Inorg. Biochem. 98, 46–60.
Okubo, T., Tanaka, N., Kim, K.H., Yone, H., Maekawa, M., Kuroda-Sowa, T., 2010. Magnetic and conducting properties of new halide-bridged mixed-valence CuI– CuII 1D coordination polymers including a hexamethylene dithiocarbamate ligand. Inorg. Chem. 49, 3700–3702.
Oladipo, S.D., Omondi, B., Mocktar, C., 2019. Synthesis and structural studies of nickel(II) and copper(II) N, N'-diarylformamidine dithiocarbamate complexes as antimicrobial and antioxidant agents. Polyhedron 170, 712–722.
Oladipo, S.D., Omondi, B., Mocktar, C., 2020. Co(III) N, N'-diarylformamidine dithiocarbamate complexes: synthesis, characterization, crystal structures and biological studies. Organomet. Chem. Appl. https://doi.org/10.1002/aoc.5610.
Oladipo, S.D., Omondi, B., 2020. Mercury(II) N, N'-diarylformamidine dithiocarbamate as single-source precursors for the preparation of oleylamine-capped HgS nanoparticles. Trans. Met. Chem. 1–12. https://doi.org/10.1007/s11243-020-00391-y.
Osowole, A.A., Kolawole, G., Fagade, O., 2008. Synthesis, characterization and biological studies on unsymmetrical Schiff-base complexes of nickel(II), copper(II) and zinc(II) and adducts with 2, 2′-dipyridine and 1, 10-phenanthroline. J. Coord. Chem. 61, 1046–1055.
Pari, L., Saravanan, R., 2004. Antidiabetic effect of diasulin, a herbal drug, on blood glucose, plasma insulin and hepatic enzymes of glucose metabolism in hyperglycaemic rats. Diabetes Obes. Metab. 6, 286–292.
Rai, M., Yadar, A., Gade, A., 2009. Silver nanoparticles as a new generation of antimicrobials. Biotechnol. Adv. 27, 76–83.
Rajput, G., Singh, V., Singh, S.K., Prasad, L.B., Drew, M.G., Singh, N., 2012. Cooperative metal–ligand-induced properties of heteroleptic copper(I) xanthate/dithiocarbamate PPh_3 complexes. Eur. J. Inorg. Chem. 2012, 3885–3891.
Ramasamy, K., Kuznetsov, V.L., Gopal, K., Malik, M.A., Raftery, J., Edwards, P.P., O'Brien, P., 2013. Organotin dithiocarbamates: single-source precursors for tin sulfide thin films by aerosol-assisted chemical vapor deposition (AACVD). Chem. Mater. 25, 266–276.
Rani, P.J., Thirumaran, S., Ciattini, S., 2014. Synthesis, spectral and antibacterial studies on Ni(II) and Zn(II) complexes involving N-furfuryl-N-isopropyldithiocarbamate (prdtc) and Lewis bases: X-ray structure of [Ni(prdtc)(NCS)(PPh_3)]. J. Sulfur Chem. 35, 106–116.
Ren, T., Lin, C., Amalberti, P., Macikenas, D., Protasiewicz, J.D., Baum, J.C., Gibson, T.L., 1998. Bis(μ-N,N'-η2-N, O-η2-N'-O-di(0-methoxyphenyl)formamidinato)disilver(I) and interesting coordination geometry for silver(I) and room temperature fluorescence.
Samouei, H., Rashidi, M., Heinemann, F.W., 2011. A cyclometalated diplatinum complex containing 1, 1′-bis (diphenylphosphino) ferrocene as spacer ligand: antitumor study. J. Organomet. Chem. 696, 3764–3771.
Sampath, K., Sathiyaraj, S., Raja, G., Jayabalakrishnan, C., 2013. Mixed ligand ruthenium(III) complexes of benzaldehyde 4-methyl-3-thiosemicarbazones with triphenylphosphine/triphenylarsine co-ligands: synthesis, DNA binding, DNA cleavage, antioxidative and cytotoxic activity. J. Mol. Struc. 1046, 82–91.
Sandroni, M., Favereau, L., Planchat, A., Akdas-Kilig, H., Szuwarski, N., Pellegrin, Y., Blart, E., Le Bozec, H., Boujtita, M., Odobel, F., 2014. Heteroleptic copper(I) polypyridine complexes as efficient sensitizers for dye sensitized solar cells. J. Mater. Chem. A 2, 9944–9947.
Sandroni, M., Kayanuma, M., Planchat, A., Szuwarski, N., Blart, E., Pellegrin, Y., Daniel, C., Boujtita, M., Odobel, F., 2013. First application of the HETPHEN concept to new heteroleptic bis (diimine) copper(I) complexes as sensitizers in dye sensitized solar cells. Dalton Trans. 42, 10818–10827.
Semeniuc, R.F., Reamer, T.J., Blitz, J.P., Wheeler, K.A., Smith, M. D., 2010. Functionalized O-alkyldithiocarbonates: a new class of ligands designed for luminescent heterometallic materials. Inorg. Chem. 49, 2624–2629.
Sheldrick, G.M., 2008. A short history of SHELX. Acta Cryst. A 64, 112–122.
Siddiqi, K., Khan, S., Nami, S.A., El-Ajaily, M., 2007. Polynuclear transition metal complexes with thiocarbohydrazide and dithiocarbamates. Spectrochim. Acta 67, 995–1002.
Soliman, A.A., Alajrawy, O.I., Attabi, F.A., Shaaban, M.R., Linert, W., 2016. New formamidine ligands and their mixed ligand

palladium(II) oxalate complexes: synthesis, characterization, DFT Calculations and in vitro cytotocity. Spectrochim. Acta A 152, 358–369.

Spek, A.L., 2009. Structure validation in chemical crystallography. Acta. Crystallogr. D Biol. Crystallogr. 65, 148–155.

Spek, A.L., 2015. PLATON SQUEEZE: a tool for the calculation of the disordered solvent contribution to the calculated structure factors. Acta Crystallorg. C Struct. Chem. 71, 9–18.

Tan, Y.S., Sudlow, A.L., Molloy, K.C., Morishima, Y., Fujisawa, K., Jackson, W.J., Henderson, W., Halim, S.N.B.A., Ng, S.W., Tiekink, E.R., 2013. Supramolecular isomerism in a cadmium bis (N-hydroxyethyl, N-isopropyldithiocarbamate) compound: physiochemical characterization of ball (n = 2) and chain (n = ∞) forms of Cd [S2CN (iPr) CH2CH2OH]2· solvent n. Cryst. Growth Des. 13, 3046–3056.

Valko, M., Rhodes, C., Moncol, J., Izakovic, M., Mazur, M., 2006. Free radicals, metals and antioxidants in oxidative stress-induced cancer. Chem.-Biol. Interact. 160, 1–40.

Vanacker, S.A., Tromp, M.N., Haenen, G.R., Vandervijgh, W., Bast, A., 1995. Flavonoids as scavengers of nitric oxide radical. Biochem. Biophys Res. Commun. 214, 755–759.

Vartale, S., Halikar, N., Pawar, Y., Tawde, K., 2016. Synthesis and evaluation of 3-cyano-4-imino-2-methylthio-4H-pyrido [1, 2-a] pyrimidine derivatives as potent antioxidant agents. Arab. J. Chem. 9, S1117–S1124.

Wang, Y.-M., Teng, F., Hou, Y.B., Xu, Z., Wang, Y.S., Fu, W.F., 2005. Copper(I) complex employed in organic light-emitting electrochemical cells: device and spectra shift. Appl. Phys. Lett. 87, 233512–233515.

Wayne, P.A., 2018. Clinical and Laboratory Standard Institue (CLSI): Performance standards for antimicrobial sucesptibility, CLSI supplement M100, 28th Edition.

Wilton-Ely, J.D., Solanki, D., Knight, E.R., Holt, K.B., Thompson, A. L., Hogarth, G., 2008. Multimetallic assemblies using piperazine-based dithiocarbamate building blocks. Inorg. Chem. 47, 9642–9653.

Xin, X.-L., Chen, M., Ai, Y.B., Yang, F.L., Li, X.L., Li, F., 2014. Aggregation-induced emissive copper(I) complexes for living cell imaging. Inorg. Chem. 53, 2922–2931.

Yang, L., McRae, R., Henary, M.M., Patel, R., Lai, B., Vogt, M.S., Fahrni, C.J., 2005. Imaging of the intracellular topography of copper with a fluorescent sensor and by synchrotron x-ray fluorescence microscopy. Proc. Ext. Met. Rev. 102, 11179–11184.